International Immunopharmacology 165 (2025) 115505

Contents lists available at ScienceDirect

International Immunopharmacology

journal homepage: www.elsevier.com/locate/intimp

Ertugliflozin ameliorates experimentally-induced colitis in rats by regulating the interplay between M1/M2 macrophage polarization, tight junction proteins, and MicroRNA 155 expression

Marina R. Fouad [a,b,*], Mostafa A. Rabie [c], Hala F. Zaki [c], Rania M. Salama [d]

[a] Postgraduate program in Pharmacology and Toxicology, Faculty of Pharmacy, Cairo University, Egypt
[b] Clinical Pharmacy Department, Faculty of Pharmacy, Misr International University (MIU), Cairo, Egypt
[c] Pharmacology and Toxicology Department, Faculty of Pharmacy, Cairo University, Cairo, Egypt
[d] Clinical Pharmacy Department, School of Pharmacy, Newgiza University, Giza, Egypt

ARTICLE INFO

Editor name: Dr. Elisabetta Liverani

Keywords:
Ulcerative colitis
Ertugliflozin
M1/M2 macrophage
Tight junction proteins
miR-155

ABSTRACT

Ulcerative colitis (UC) is a persistent inflammatory condition marked by the destruction of the intestinal mucosal barrier, infiltration of inflammatory cells, and ulceration. M1/M2 macrophage polarization plays an imperative function in the regulation of inflammation through the nuclear factor-kappa B (NFκB) signaling pathway and modulating microRNA-155 (miR-155). Recent studies have highlighted the anti-ulcerogenic and colo-protective properties of sodium-glucose co-transporter-2 (SGLT2) inhibitors. However, the potential protective and therapeutic effects of ertugliflozin (Ertu), an SGLT2 inhibitor, in UC have not yet been clarified. Therefore, the present research sought to investigate the potential role of Ertu in mitigating acetic acid (AA)-induced UC in rats. Forty-two adult Wistar rats were allocated into seven groups: control, Ertu (10 mg/kg), AA, AA+ Ertu (1, 5, and 10 mg/kg), and AA+ sulfasalazine (Sulfa) (100 mg/kg); all received oral treatments daily for 7 days. Pre-treatment with Ertu mitigated histopathological alterations and enhanced macroscopic assessments. Ertu suppressed the expression of NF-κB p65 and miRNA-155, promoting macrophage polarization towards M2 phenotype, as witnessed by increased expression of CD206, Fizz-1, Ym-1, and Arg-1, along with elevated IL-10 protein content. It reduced the expression of CD86 and MCP-1, besides the levels of TNF-α, IL-1β and iNOS. Moreover, Ertu improved intestinal epithelial integrity by upregulating tight junction proteins, comprising claudin-1, occludin and ZO-1. Ertu also demonstrated anti-apoptotic effects by reducing BAX meanwhile increasing BCL2. Notably, Ertu (10 mg/kg) exhibited therapeutic effects comparable to the standard treatment, Sulfa, underscoring its potential as a distinctive and valuable option for UC management.

1. Introduction

Ulcerative colitis (UC) is listed among the conventional prevalent inflammatory bowel diseases that cause persistent inflammation in the innermost lining of the colon and rectum [1], leading to significant impairment of patients' well-being and an increased risk of colon cancer [2]. Weight loss, fluid and electrolyte imbalances, bloody diarrhea, and colonic pain are clinical signs of UC [3]. Symptoms usually occur in sporadic episodes, which can increase in frequency over time and, in some cases, become severe enough to necessitate hospitalization [4,5].

Abbreviations: AA, acetic acid; Akt, protein kinase B; AMPK, AMP-activated protein kinase; Arg-1, arginase-1; BAX, BCL2-associated X protein; BCL2, B-cell lymphoma 2; CD, cluster of differentiation; DAI, disease activity index; Ertu, ertugliflozin; Fizz-1, found in inflammatory zone-1; GI, gastrointestinal; H&E, Hematoxylin and Eosin; iNOS, inducible nitric oxide synthase; IL, interleukin; MCP-1, monocyte chemoattractant protein-1; MDA, malondialdehyde; miR-155, microRNA 155; pS536, NFκB p65; phospho-serine, 536 nuclear factor-kappa B; SGLT2, sodium-glucose co-transporter-2; SOD, superoxide dismutase; Sulfa, sulfasalazine; TJ, tight junction; TNF-α, tumor necrosis factor-alpha; TLR4, toll-like receptor 4; UA, ulcer area; UC, ulcerative colitis; UI, ulcer index; Ym-1, chitinase-3-like protein 1; ZO-1, zonula occludens-1.

* Corresponding author at: Clinical Pharmacy Department, Faculty of Pharmacy, Misr International University, Km 28 Cairo-Ismailia Road (Ahmed Orabi District), Cairo, Egypt.

E-mail addresses: marina.pharmacist@miuegypt.edu.eg (M.R. Fouad), mostafa.mohammed@pharma.cu.edu.eg (M.A. Rabie), hala.fahmy@pharma.cu.edu.eg (H.F. Zaki), rania.salama@ngu.edu.eg (R.M. Salama).

https://doi.org/10.1016/j.intimp.2025.115505
Received 7 March 2025; Received in revised form 1 September 2025; Accepted 2 September 2025
Available online 6 September 2025

A significant number of UC patients also develop extraintestinal manifestations, affecting various organs and exhibiting characteristics similar to those seen in other autoimmune diseases. Actually, two major sites of extra-colonic gastrointestinal (GI) involvement are the pancreas and the hepatobiliary system, whereas the most frequently affected non-GI systems include the musculoskeletal, ocular, and renal systems. [4]. Although the exact culprit of UC stays elusive, it is thought to arise from a blend of environmental factors, genetic predispositions, gut microbiota and immune system dysfunctions [5,6]. Besides, research indicates that variations among ethnic and racial groups are primarily influenced by environmental factors, dietary patterns, and lifestyle choices, rather than actual genetic differences [4]. A key factor in the pathogenesis of UC is the disruption of the GI mucosal barrier, which increases intestinal permeability and allows harmful pathogens and toxins to penetrate the epithelial layer [5,7].

Acetic acid (AA) induced colitis is one of the most frequently used and readily inducible murine models, closely mimicking the pathogenesis, histological features, and immune responses observed in human UC. It is characterized by extensive necrosis of the mucosal and submucosal layers, along with vascular dilation, edema, and ulceration, followed by neutrophil infiltration. Noteworthy, AA causes direct epithelial injury and initiates a robust inflammatory response. The latter is mediated by the activation of proinflammatory cytokines and oxidative stress pathways, both of which play central roles in UC pathogenesis [8–10]. At the mechanistic level, AA penetrates the epithelial barrier and disperses protons into intracellular compartments, leading to local acidification. This process disrupts cellular integrity and triggers a cascade of tissue damage and inflammation that mirrors the pathological features of UC [11,12].

Tight junction (TJ) proteins, comprised of transmembrane proteins including occludins and claudins, along with accessory proteins like zonula occludens, play a fundamental function in preserving the epithelial barrier's integrity by connecting epithelial cells [13]. Consequently, therapies that regulate TJ proteins and strengthen the epithelial barrier are critical for effective UC treatment. In parallel, macrophages have a crucial function in the immunological response and cytokine signaling in UC [14]. These immune cells can polarize into two main phenotypes: pro-inflammatory M1-like macrophages, which produce mediators like tumor necrosis factor-alpha (TNF-α), inducible nitric oxide synthase (iNOS) and interleukin-1 beta (IL-1β), thereby exacerbating inflammation, and anti-inflammatory M2-like macrophages, characterized by the manifestation of indicators like arginase-1 (Arg-1), chitinase-like 3 (Ym-1), and interleukin-10 (IL-10), which suppress inflammation and promote tissue repair [15]. Noteworthy, microRNA 155 (miR-155) is upregulated in UC, favoring M1 polarization by stimulating the nuclear factor-kappa B (NFκB) cascade while inhibiting M2 polarization [14,16]. Therefore, targeting miR-155 to stimulate macrophages to adopt the anti-inflammatory M2 phenotype instead of the pro-inflammatory M1 phenotype signifies a promising therapeutic approach for managing UC.

Despite the absence of a definitive cure for UC, several FDA-approved medications are available to manage the condition. Sulfasalazine (Sulfa) was the first antibiotic introduced for UC treatment, primarily due to its combined antibacterial and anti-inflammatory properties. However, the widespread use of traditional medications has been limited by challenges such as reduced long-term efficacy, undesirable side effects, and dosage complexities [17]. Due to the limitations linked to UC therapies, alternative treatment approaches are under investigation and are advancing into clinical trials such as anti-integrin, anti-IL-23, sphingosine-1-phosphate receptor modulator and fecal microbiota transplant [18]. Additionally, phosphodiesterase enzyme 4 inhibitors as ibudilast evidenced to have a momentous role in the management of UC [19]. However, serious flare-ups may require hospital admission and administration of steroids through intravenous therapy [20]. Hence, there is a necessity for the manifestation of safer and more effective curative options for UC.

Sodium-glucose co-transporter-2 (SGLT2) inhibitors, commonly referred to as gliflozins, represent a novel family of anti-diabetic drugs [21] designed to reduce levels of glucose in the blood by increasing urinary glucose excretion. Beyond their hypoglycemic effects, these drugs exhibit notable renal and cardioprotective benefits with emerging potential impacts on cerebral tissues [3]. Interestingly, SGLT2 is widely expressed in the GI tract, primarily in the small and large intestines [22]. Recent studies suggest that SGLT2 inhibitors, for instance canagliflozin, dapagliflozin, and empagliflozin, may serve as promising therapeutic agents for UC. In animal models, these drugs have been shown to significantly attenuate inflammation, oxidative stress, and apoptosis while reducing colonic injury [21,23,24]. Their anti-inflammatory properties were attributed to the modulation of innate immune cells, suppression of pro-inflammatory cytokine expression, and inhibition of inflammasome activation. Moreover, gliflozins enhance colonic barrier function, contributing to their anti-ulcerogenic and colo-protective actions [3,23]. In addition, SGLT2 inhibitors have demonstrated beneficial effects not only in the management of UC but also in a range of other immune-mediated diseases through modulating immune responses, reducing inflammatory cytokine production, and attenuating tissue damage. These findings suggest a broader therapeutic potential for SGLT2 inhibitors in treating autoimmune and inflammatory disorders beyond their primary use in metabolic diseases [25–27]. On the other hand, SGLT2 inhibitors are generally well tolerated but they are associated with several notable adverse effects, most commonly genital mycotic infections, increased urination, volume depletion, urinary tract infections, and ketoacidosis [28]. These findings highlight the prospects of SGLT2 inhibitors as an innovative approach for UC treatment.

Ertugliflozin (Ertu) is a selective and potent SGLT2 inhibitor, permitted by the U.S. Food and Drug Administration and European Medicines Agency for the treatment of type 2 diabetes at daily doses of 5 mg and 15 mg [29,30]. It is a safe and effective oral medication for patients over 18, used alongside diet and exercise, with over 2000-fold higher selectivity for SGLT2 compared to SGLT1 [31]. Beyond glucose control, Ertu has demonstrated cardiovascular benefits by improving left ventricular remodeling and reducing apoptosis and endoplasmic reticulum stress in an experimental model of cardiac pressure overload, primarily through the stimulation of protein kinase B (Akt) and downregulation of caspase-3, collagen I, and IL-1β [32]. Additionally, Ertu attenuated oxidative stress [33] and demonstrated a neuroprotective effect in rats by upregulating Akt and the anti-apoptotic protein B-cell lymphoma 2 (BCL2), along with suppression of pro-apoptotic proteins, including BCL2-associated X protein (BAX) and cleaved caspase-3 [34]. However, its role in UC has not been yet clarified. Thus, the current research aims to explore the potential advantageous outcomes of Ertu in combating experimentally induced UC in rats, and the underlying molecular mechanism involved.

2. Materials and methods

2.1. Ethics statement

The study commenced after receiving approval for the study protocol from Cairo University's Faculty of Pharmacy's Ethics Committee for Animal Experimentation (Permit Number: PT 3116). Furthermore, all procedures adhered to ethical guidelines outlined in the Guide for the Care and Use of Laboratory Animals [35], ensuring minimal animal distress.

2.2. Animals

Forty-two adult male and female Wistar rats weighing ≈ 180–220 g were obtained from the animal facility of the National Research Centre (Cairo, Egypt). The rats were permitted for a week to acclimatize at the animal facility, kept in standard cages made of polypropylene with four rats per cage. The cages used in the experiment were large and

segmented so as each rat was housed alone in separate partition to decrease the contact between rats and to avoid licking or grooming behaviors that could interfere with the colitis model or treatment outcomes. Also, cages were regularly cleaned, and animals were monitored daily to ensure well-being and minimize stress. During the entire experiment, rats had ad libitum access to a normal pellet diet (Meladco, Cairo, Egypt) and tap water. They were maintained under controlled conditions, including a temperature of 22 ± 2 °C, relative humidity of 55 ± 5 %, and a 12-h light/12-h dark cycle.

2.3. Induction of ulcerative colitis

Animals were deprived of food for 24 h prior to colitis induction while being allowed free access to tap water. However, water access was restricted two hours before the experiment. Colonic inflammation was induced under ketamine anesthesia (50 mg/kg, i.p.), via the administration of 2 ml of 4 % acetic acid (AA) in 0.9 % NaCl intra-rectally, utilizing a 2 mm diameter silicone catheter, implanted 8 cm into the colon. To prevent leakage, the rats were held upright for 2 min. Control animals endured the same procedure, but using 0.9 % NaCl in place of solution of the AA [36,37].

2.4. Experimental design

Ertu was obtained from Hikma Pharmaceuticals (Giza, Egypt). Ertu was dissolved in normal saline 0.9 % to reach a final concentration of 1 mg/ml and given at doses of 1, 5 and 10 mg/kg [34,38,39]. Sulfa was obtained from Kahira Pharmaceuticals & Chemical Industries Co. (Cairo, Egypt) was dissolved in normal saline 0.9 % to reach a final concentration of 10 mg/ml and given at the dose of 100 mg/kg [40]. Unless specified otherwise, all chemicals and solvents used in the study were of the highest analytical grade and sourced from reputable suppliers.

As presented in the experimental timeline design (Fig. 1), Forty-two rats were allocated into 7 groups using simple random sampling ($n = 6$ rats/group), and the study was conducted for 7 days along these lines:

Group I: Animals were given saline 10 ml/kg orally daily to act as a normal control group.
Group II: Animals were given Ertu 10 mg/kg orally daily to act as a drug control group [34,38].
Group III: Animals were given saline 10 ml/kg orally daily from day 1 to day 7, with intrarectal administration of a single dose of 2 ml of 4 % AA on day 4 for induction of UC, to be nominated as UC group [41,42].
Group IV: Animals were orally pre-treated with Ertu 1 mg/kg daily from day 1 to day 7, with intrarectal administration of a single dose of 2 ml of 4 % AA on day 4 for induction of UC [38].
Group V: Animals were orally pre-treated with Ertu 5 mg/kg daily from day 1 to day 7, with intrarectal administration of a single dose of 2 ml of 4 % AA on day 4 for induction of UC [34,39].
Group VI: Animals were orally pre-treated with Ertu 10 mg/kg daily from day 1 to day 7, with intrarectal administration of a single dose of 2 ml of 4 % AA on day 4 for induction of UC [34,38].
Group VII: Animals were orally pre-treated with Sulfa 100 mg/kg daily from day 1 to day 7, with intrarectal administration of a single dose of 2 ml of 4 % AA on day 4 for induction of UC [40].

By the end of the experimental period, rats were fasted overnight, and on day 8 (Twenty-four hours after the last administered treatment). For anesthetization, an intraperitoneal injection of 50 mg/kg ketamine hydrochloride and 5 mg/kg xylazine was used [43]. Before euthanasia, blood samples were collected via the retro-orbital plexus. Sera was isolated by centrifuging the samples at 3000 rpm for 15 min and then preserved at −80 °C for subsequent glucose level analysis. After

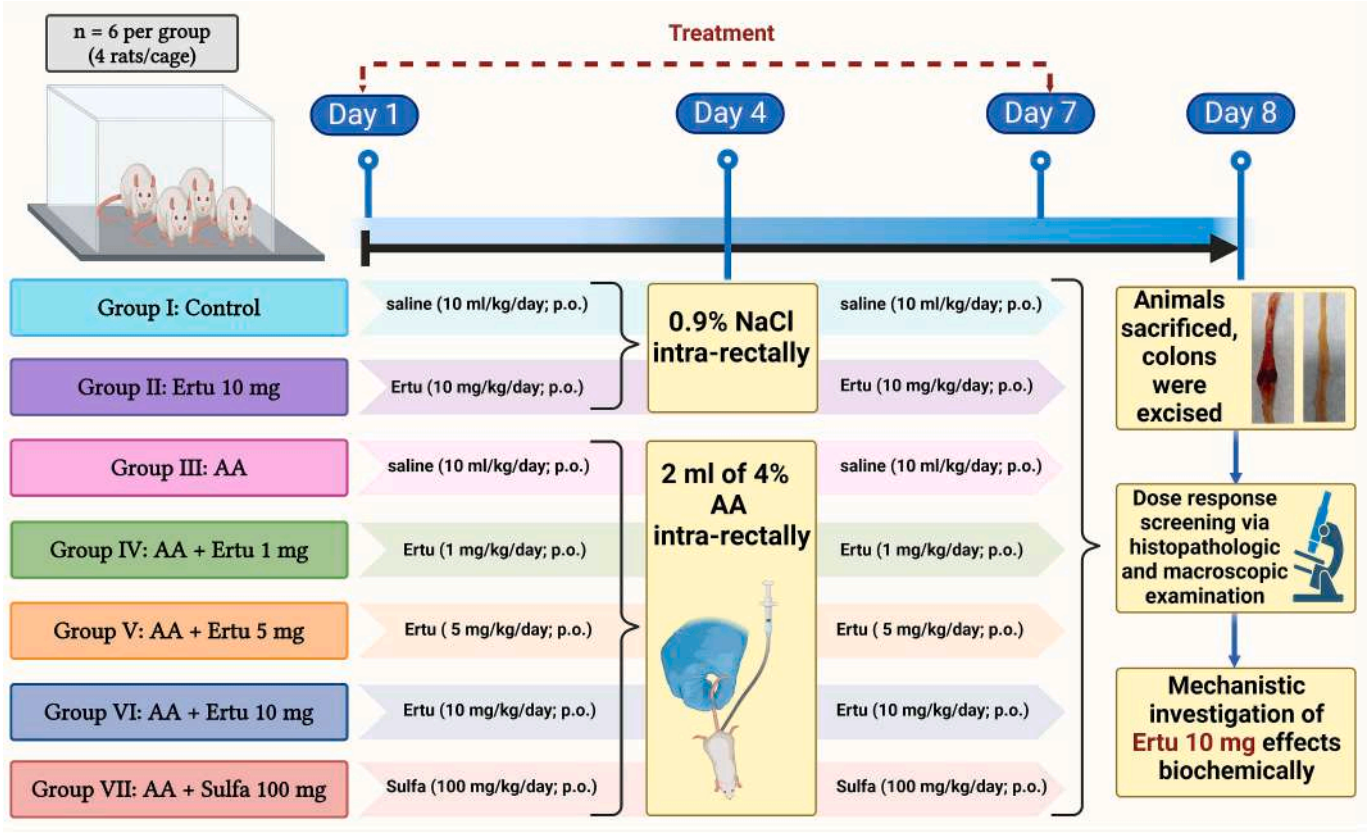

Fig. 1. Experimental timeline, designed through BioRender.com, for the exploration of the colo-protective and therapeutic upshots of ertugliflozin (Ertu) in comparison to the standard drug sulfasalazine (Sulfa) in combating ulcerative colitis (UC) induced by acetic acid (AA) in rats.

euthanasia, the colons were excised, opened longitudinally, cleaned of luminal contents, rinsed with phosphate-buffered saline, and dried. Colitis was evaluated macroscopically by measuring the colon's weight, length, and diameter, and recording ulcer number and area. A 5-cm section of each colon was fixed in 10 % formalin for histopathological investigation, meanwhile, the remaining colon tissue was preserved at −80 °C for biochemical assays. All evaluations were conducted blindly.

The dose-dependent colo-protective upshots of Ertu at the doses of 1, 5 and 10 mg/kg were initially assessed based on histopathological examination using Hematoxylin and Eosin (H&E) and Alcian blue stains along with the macroscopic assessment. Accordingly, the best protective dose of Ertu was further assessed by biochemical analysis to divulge the functional outcomes of Ertu.

2.5. Methods

2.5.1. Disease activity index (DAI)

The calculation of the disease activity index (DAI) depends on the summed values for the percentage of body weight loss with a score from 0 to 4, stool consistency with a score from 0 to 4, and rectal bleeding with a score from 0 to 4, and subsequently divided by 3 as formerly reported [37,44]. DAI was determined based on the equation below:

$$\text{DAI} = \frac{\text{body weight loss score} + \text{diarrhea score} + \text{rectal bleeding score}}{3.}$$

Daily weight changes were monitored and recorded during the experiment and body weight loss was estimated as the percentage change compared to the pre-UC induction (Day 4) body weight and the final body weight prior to euthanasia (Day 8). Additionally, each animal's fecal samples were daily examined visually for indications of rectal bleeding and diarrhea. The scoring of stool consistency was along these lines, normal (0), loose stool (1 & 2) besides diarrhea (3 & 4). The existence of occult blood in feces was detected by a benzidine test [45]. The acquired score for Occult blood was 0, for no change in color; 1 (±), for faint blue color that developed after more than 30 s; 2 (+), for a blue color that appeared within 30 s or longer; 3 (++), for an immediate color change that occurred in less than 30 s; whereas 4, for gross blood visible on the slide **(**Table 1**)**.

2.5.2. Colon mass index (mg/g)

The colon mass index, defined as the colon weight-to-body weight ratio, expressed as milligrams per gram, was used as an indicator to assess the degree of colonic inflammation severity and the extent of colonic edema [46].

2.5.3. Ratio of colon weight to length (g/cm)

The ratio of colon weight to length was calculated to verify the severity of colitis using the following equation [40,47]:

$$\text{Ratio of colon weight to length} = \frac{\text{colon weight (g)}}{\text{colon length (cm)}}$$

2.5.4. Ulcer area (UA) and ulcer index (UI)

A magnifying lens (x10) was used to evaluate and quantify the ulcer area (UA) in colonic lesions, while the ulcer index (UI) was computed using the formula below, as formerly stated [48].

$$\text{UI} = \frac{\text{Total area of the ulcer (mm}^2\text{)}}{\text{Total area of the colon specimen (mm}^2\text{)}}$$

Subsequently, the average lesion score for all rats was recorded and used to estimate each group's UI. Additionally, the inhibition percentage was calculated by means of the following equation, as described in an earlier study [44].

$$\text{Inhibition\%} = \frac{\text{UI of AA group} - \text{UI of Ertu or Sulfa groups}}{\text{UI of AA group}} \text{ x } 100$$

2.5.5. Colonic damage scoring

The macroscopic characteristics of UC in rats were evaluated using a previously established scoring system [49,50], with ratings between 0 and 4:

(0) Absence of macroscopic alterations.

(1) Only mucosal erythema.

(2) The presence of mild mucosal edema, slight bleeding or minor erosions.

(3) Moderate edema, slight bleeding ulcers or erosions.

(4) Severe edema, ulceration and tissue necrosis.

2.5.6. Biochemical assays

2.5.6.1. Measurement of glucose levels in serum. The glucose oxidase/peroxidase method [51] was used to colorimetrically measure the serum glucose by utilizing Thermo Fisher Glucose Colorimetric Detection Kit (MA, USA).

2.5.6.2. Western blot analysis. Electrophoresis was executed on samples with equivalent protein levels (≈ 20 μg) utilizing 10 % sodium dodecyl sulfate-polyacrylamide gel (SDS-PAGE), followed by electro-transfer onto polyvinylidene difluoride membranes. For 2 h at room temperature, blocking of the membranes was performed using 5 % (*w/v*) skim milk powder dissolved in phosphate-buffered saline with Tween-20. The membranes were then incubated with the following polyclonal antibodies, purchased from Thermo Fisher Scientific (MA, USA), each diluted 1:1000 in Tris-buffered saline with Tween (TBST) containing 1 % bovine serum albumin: pS536-NFκB p65 (catalog # PA5–121262, RRID AB_2914834), total NFκB p65 (catalog # PA5–27617, RRID AB_2545093), cluster of differentiation 86 (CD86) (catalog # PA5–79009, RRID AB_2746125), cluster of differentiation 206 (CD206) (catalog # PA5–101657, RRID AB_2851091), monocyte chemoattractant protein-1 (MCP-1) (catalog # PA5–115555, RRID AB_2893318), arginase-1 (Arg-1) (catalog # PA5–85267, RRID AB_2792410), chitinase-3-like protein 1 (CHI3L1/Ym-1) (catalog # PA5–37357, RRID AB_2554024), found in inflammatory zone-1 (Fizz-1) (catalog # BS-1884R, RRID AB_10855574), claudin-1 (catalog # 51–9000, RRID AB_2533916), occludin (catalog # 40–4700, RRID AB_2533468), and zonula occludens-1 (ZO-1) (catalog # 61–7300, RRID AB_2533938). β-actin (Santa Cruz Biotechnology, TX, USA) was used as an internal control, also diluted 1:1000 in the blocking buffer. After an hour of room temperature incubation with the relevant secondary antibodies, the membranes were washed and developed. Lastly, densitometric measurement was carried out utilizing Image J software (Bio-Rad, CA, USA) after images of the appropriate protein bands were captured on the BioMax film (Kodak). Band densities were standardized to match the density of β-actin or total protein.

2.5.6.3. Determination of relative expression of colonic miR-155, claudin-1, occludin, and ZO-1 by real-time PCR. For total RNA extraction from homogenized rat colonic tissue, a Qiagen tissue extraction kit (Qiagen Sciences Inc., MD, USA) was utilized. The tissue lysates were then centrifuged for 3 min at 10,000 ×g. Following the manufacturer's

Table 1
Disease activity index (DAI).

DAI Score	%weight loss	Stool consistency	Occult/gross bleeding
0	None	Normal	Negative
1	1–5 %	Loose stool	Occult blood ±
2	>5–10 %		Occult blood +
3	>10–15 %	Diarrhea	Occult blood ++
4	>15 %		Gross blood

(±) faint blue color that developed after more than 30 s; (+) for a blue color that appeared within 30 s or longer; (++) for an immediate color change that occurred in less than 30 s.

instructions, the supernatants were gathered and reverse-transcribed into cDNA via a high-capacity cDNA reverse transcription kit (Applied Biosystems, CA, USA). SYBR® Green PCR Master Mix (Applied Biosystems, CA, USA) was used in quantitative real-time PCR aligned with the manufacturer's recommendations to evaluate the expression of the target genes claudin-1, occludin, and zonula occludens-1 (ZO-1). The formerly reported ΔΔ CT technique [52] was implemented to gauge the absolute target gene expression. Besides, β-actin was employed as a gene for housekeeping.

Colonic tissue homogenate was processed to extract total miRNA utilizing the mirVana™ miRNA isolation kit (Ambion®, TX, USA) and subsequently reverse-transcribed into cDNA following the manufacturer's protocol with the miRCURY LNA miRNA RT kit (Qiagen, Hilden, Germany). MiRNA levels were quantified from cDNA using real-time PCR, following the manufacturer's protocol with the miRCURY SYBR® Green PCR Kit (Qiagen, Hilden, Germany). Finally, the formerly reported ΔΔ CT technique [52] was used to analyze the absolute expression of miRNA. Besides, U6 was employed as a gene for housekeeping **(**Table 2**)**.

2.5.6.4. Determination of mediators of colonic inflammation, oxidative stress and apoptosis. The colonic levels of TNF-α (Catalog # CSB-E11987r, detection range spans 6.25 to 400 pg/ml, the sensitivity is 1.56 pg/ml, the intra-assay precision is CV < 8 % and the inter-assay precision is CV < 10 %), IL-1β (Catalog # CSB-E08055r,detection range spans 31.25 to 2000 pg/ml, the sensitivity is 15.6 pg/ml, the intra-assay precision is CV < 8 % and the inter-assay precision is CV < 10 %), IL-10 (Catalog # CSB-E04595r detection range spans 3.12 to 200 pg/ml, the sensitivity is 0.78 pg/ml, the intra-assay precision is CV < 8 % and the inter-assay precision is CV < 10 %), BAX (Catalog # CSB-EL002573RA, detection range spans 62.5 to 4000 pg/ml, the sensitivity is 15.6 pg/ml, the intra-assay precision is CV < 8 % and the inter-assay precision is CV < 10 %), and BCL2 (Catalog # CSB-E08854r, detection range spans 312 to 20,000 pg/ml, the sensitivity is 78 pg/ml, the intra-assay precision is CV < 8 % and the inter-assay precision is CV < 10 %) were determined using Cusabio rat ELISA kits (Wuhan, China). While iNOS (Catalog # EEL132, detection range spans 0.31to 20 ng/ml, the sensitivity is 0.19 ng/ml, the intra-assay precision is CV < 10 % and the inter-assay precision is CV < 10 %), was determined using Thermo Fisher Scientific; MA; USA kit. All procedures were conducted in a manner that aligned with the manufacturer's protocols. The results were standardized to protein content, which was quantified utilizing the Bradford method of protein estimation Bradford [53].

Also, oxidative stress markers, such as MDA (Catalog # *E*-BC-K025-S, detection range spans 0.38 to 133.33 nmol/ml, the sensitivity is 0.38 nmol/ml, the intra-assay precision is CV < 4.9 % and the inter-assay precision is CV < 8 %) and SOD (Catalog # EIASODC, detection range spans 1.4 to 92 U/ml, the sensitivity is 0.044 U/ml, the intra-assay precision is CV < 10 % and the inter-assay precision is CV < 12 %) were determined by colorimetric assay following the manufacturer's protocol using available commercial kits. MDA is expressed as nmol per mg protein (Elabscience Biotechnology Inc. Wuhan, China) while SOD is expressed as unit per mg protein (Thermo Fisher Scientific; MA; USA).

Table 2
Forward and reverse primers for quantitative RT-PCR.

Gene	GenBank accession number	Primer Sequence 5′–3′
miR-155	NR_106710.1	F: TGTGATAGGGGTTTTGGCCTC R: TGTTAATGCTAACAGGTAGGAGTC
Claudin-1	**NM_031699.3**	F: TGGGGCTGATCGCAATCTTT R: ACTTAAGGAGCACCCTTCGC
Occludin	**NM_031329.3**	F: TGTGTTCCCCCAGGTAGACT R: GGTCACACAGTGACACTCCA
ZO-1	**NM_001106266.1**	F: TCGGAGCTCGGGCATTATTC R: CAGGGCACCATACCAACCAT
U6	**K00784.1**	F: CTCGCTTCGGCAGCACA R: AACGCTTCACGAATTTGCGT
β-actin	**NM_031144**	F: GGTCGGTGTGAACGGATTTGG R: ATGTAGGCCATGAGGTCCACC

2.5.7. Histopathological evaluation

Samples of colonic tissue were flushed and preserved for 72 h in 10 % neutral buffered formalin. After trimming, the samples underwent processing through serial ethanol concentrations, then treated with xylene for clearing and embedded within Paraplast® tissue embedding media. Tissue sections, 5 μm thick, were cut using a rotatory microtome to illustrate the intestinal wall. H&E staining was performed for general morphology, while Alcian Blue (pH 2.5) was utilized to identify goblet cells and acidic mucins. An experienced histologist conducted the examination following standard fixation and staining protocols [54]. Based on Khedr et al., [55], a minimum of six randomly selected non-overlapping fields were scanned for analysis, assessing mucosal region percentages of goblet cell mucin content and average goblet cell counts in sections stained with Alcian Blue. A Full HD microscopic imaging system (Leica Microsystems GmbH, Germany) equipped with the Leica Application module was utilized to collect histological data.

2.6. Statistical analysis

The Shapiro-Wilk test was used to assess the normality of each variable, confirming a normal distribution. Consequently, parametric analyses were conducted, and data were expressed as means ± SD. Group comparisons were analyzed through one-way ANOVA, succeeded by Tukey's post hoc test, with statistical significance set at $p < 0.05$. All data processing and statistical evaluations were performed using GraphPad Prism® (Version 9.10, CA, USA).

3. Results

The analysis of statistics indicated the absence of significant differences between the normal (Gp 1) and the drug (Gp 2) control groups across all assessed parameters, thus comparisons were made relative to the normal control group (Gp 1) only. Moreover, there was no mortality noted in any of the animal groups. Notably, serum glucose levels were normal across all groups with no significant differences observed, leading to the exclusion of glucose data from analysis (Table 3**)**.

3.1. Effect of Ertu 1, 5, and 10 mg/kg on macroscopic examination features of UC

3.1.1. Disease activity index (DAI)

Animals that received AA exhibited a significant upsurge in DAI by 4.6-fold in comparison to the control group [F (6,35) = 21.81]. On the other hand, administration of Ertu at 1, 5, and 10 mg/kg caused a significant decline in DAI by 33 %, 33 %, and 35 %, respectively, relative to the AA group. Likewise, Sulfa (100 mg/kg) treatment revealed a 30 % significant diminution in DAI in comparison to the AA group **(**Table 4**)**.

Table 3
Effect of ertugliflozin on serum glucose levels of acetic acid-induced colitis in all rat groups.

	Control	Ertu 10 mg	AA	AA+ Ertu 1 mg	AA+ Ertu 5 mg	AA+ Ertu 10 mg	AA+ Sulfa 100 mg
Serum glucose (mg/dl)	137 ± 11.6	137 ± 11.8	121 ± 24.7	130 ± 10.9	134 ± 23.9	137.6 ± 17.9	128 ± 13.5

Values symbolize the mean ± SD ($n = 6$ per group; one-way ANOVA succeeded by Tukey's post hoc test. AA, acetic acid; DAI, disease activity index; Ertu, ertugliflozin; Sulfa, sulfasalazine; UC, ulcerative colitis; UI, ulcer index.

Table 4
Macroscopic effects of ertugliflozin on acetic acid-induced ulcerative colitis in rat groups.

Groups	DAI	Colon mass index (g/cm)	Colon weight/length ratio (g/cm)	UI	Inhibition %	Macroscopic Scoring
Control	0.72 ± 0.20	7.63 ± 0.45	0.07 ± 0.01	0.00 ± 0.00	–	0.00 ± 0.00
Ertu 10 mg	0.68 ± 0.14	7.67 ± 0.34	0.07 ± 0.008	0.00 ± 0.00	–	0.00 ± 0.00
AA	3.41 ± 0.24****	9.51 ± 0.55**	0.14 ± 0.01****	0.10 ± 0.07****	–	3.66 ± 0.51****
AA+ Ertu 1 mg	2.28 ± 0.54##	7.99 ± 0.74#	0.09 ± 0.01####	0.02 ± 0.02##	80 %	2.33 ± 0.81##
AA+ Ertu 5 mg	2.27 ± 0.67##	7.76 ± 1.14##	0.08 ± 0.01####	0.007 ± 0.01###	93 %	1.33 ± 0.51####
AA+ Ertu 10 mg	2.20 ± 0.79##	7.82 ± 0.70##	0.09 ± 0.01####	0.009 ± 0.006###	91 %	1.50 ± 0.54####
AA+ Sulfa 100 mg	2.37 ± 0.55#	8.16 ± 0.74#	0.10 ± 0.01###	0.01 ± 0.02##	90 %	2.00 ± 0.89###

Values symbolize the mean ± SD ($n = 6$ per group; one-way ANOVA succeeded by Tukey's post hoc test; ** $p < 0.01$, vs. the control group; **** $p < 0.0001$, vs. the control group; # $p < 0.05$, vs. AA treated group; ## $p < 0.01$, vs. AA treated group; ### $p < 0.001$, vs. AA treated group; #### $p < 0.0001$, vs. AA-treated group). AA, acetic acid; DAI, disease activity index; Ertu, ertugliflozin; Sulfa, sulfasalazine; UC, ulcerative colitis; UI, ulcer index.

3.1.2. Colon mass index (mg/g)

As depicted in Table 4, AA increased colon mass index by 1.2-fold in comparison to the control group [F (6,35) = 5.081]. In contrast, doses of Ertu at 1, 5, and 10 mg/kg succeeded in reducing colon mass index by 16 %, 18 %, and 18 %, respectively as compared to the insult. In the same context, Sulfa (100 mg/kg), the standard treatment, displayed a 14 % decrease in colon mass index as compared to the insult.

3.1.3. Ratio of colon weight to length (g/cm)

Acetic acid injection triggered a significant escalation in the ratio of colon weight to length by 1.9-fold in comparison to the control group [F (6,35) = 16.25]. Contrariwise, pre-treatment with Ertu (1, 5, and 10 mg/kg) displayed an obvious decline in the ratio of colon weight to length by 34 %, 42 %, and 36 %, respectively, relative to the AA group. Similarly, Sulfa treatment (100 mg/kg) caused a 29 % decrease in the ratio of colon weight to length, relative to the AA group **(**Table 4**)**.

3.1.4. Ulcer index (UI) and Inhibition %

Animals that received AA showed a noticeable increase in UI in comparison to the control group [F (6,35) = 7.928]. On the other hand, pre-treatment with Ertu 1, 5, and 10 mg/kg reduced UI by 80-, 93- and 91 %, respectively, relative to the AA group. In the same line, the administration of Sulfa (100 mg/kg) diminished UI by 90 %, relative to the AA group **(**Table 4**)**.

3.1.5. Colonic damage scoring

As illustrated in Table 4, the macroscopic scoring of colonic damage of the dissected colon showed an obvious boost in AA-treated animals relative to the control group [F (6,35) = 30.89]. Alternatively, the administration of Ertu at 1, 5, and 10 mg/kg succeeded in reducing the colonic damage score by 36 %, 64 %, and 59 %, respectively, in comparison to the insult. Similarly, pre-treatment with Sulfa (100 mg/kg) lessened the colonic damage score by 45 %, relative to the AA group.

3.2. Effect of Ertu 1, 5, and 10 mg/kg on histopathological investigation

Microscopic analysis of H&*E*-staining colon tissues from both normal controls **(**Fig. 2A **& a)** and drug control **(**Fig. 2B & b**)** groups demonstrated normal, well-preserved architecture. The colon wall was intact with well-structured colonic crypts, abundant goblet cells, and a healthy epithelial lining. The submucosal and outer muscular layers appeared normal without any abnormalities.

In contrast, colon sections of the AA group **(**Fig. 2C & c**)** exhibited ulcerative hemorrhagic colitis with severe mucosal necrosis, leading to the loss of normal colonic wall architecture and the disappearance of glandular structures. These pathological changes were accompanied by moderate to severe mixed inflammatory cell infiltration in the submucosa and mucosa, as well as congested blood vessels and significant submucosal edema.

Notably, pre-treatment with a low dose of Ertu (1 mg/kg) revealed mild shielding effects, though some mucosal ulceration and epithelial loss were present. Areas of re-epithelialization of glandular structures were noted, but the presence of mature goblet cells was limited, accompanied by a significant infiltration of mixed inflammatory cells **(**Fig. 2D & d**)**.

In contrast, the medium- (5 mg/kg) and high-dose (10 mg/kg) Ertu groups, as well as the group treated with Sulfa (100 mg/kg), exhibited obvious enhancement in histological organization. These groups exhibited restoration of the colonic wall, with intact epithelial linings and well-formed mucosal glands. The number of mature goblet cells increased significantly. However, the medium-dose Ertu (5 mg/kg) showed occasional focal necrosis in the mucosal layer, with some inflammatory cell infiltration into the submucosa (Fig. 2E & e). The Sulfa group had moderate levels of persistent inflammation in the mucosa and submucosa, along with mild submucosal edema and congested blood vessels **(**Fig. 2G & g**)**. In the high-dose Ertu group, there was a marked reduction in inflammatory cells, with only mild infiltration and moderate vascular congestion **(**Fig. 2F & f**)**.

3.3. Effect of Ertu 1, 5, and 10 mg/kg on mucosal goblet cell counts and the acidic mucin content in colonic tissues stained with Alcian blue

As revealed in Fig. 3, AA-induced a significant drop in the goblet cell count by 87.1 %, in comparison to the control group [F (6,35) = 237.9]. Whereas treatment with Ertu (1, 5, and 10 mg/kg), as well as Sulfa (100 mg/kg), displayed an increase in goblet cell counts within the colon by 2.9-, 3.-8, 6.3-, and 5.4-fold, respectively, relative to AA group. Notably, Ertu (10 mg/kg) resulted in the highest increase in goblet cell count compared to all other groups.

Similarly, colonic acidic mucin content demonstrated a significant decline in the AA group by 83.5 %, in comparison to the normal control group [F (6,35) =223]. However, treatment with Ertu (1, 5, and 10 mg/kg) in addition to Sulfa-treated group (100 mg/kg) displayed a significant enhancement in mucin content within the colon by 2.8-, 3.8-, 4.4-, and 3.6-fold, respectively, in comparison to AA group. Noteworthy, Ertu (10 mg/kg) exhibited the greatest increase in mucin content compared to the other groups.

Notably, the initial dose-response investigation evaluated the protective effects of Ertu at three dose levels (1, 5, and 10 mg/kg) using DAI, colon mass index, ratio of colon weight to length, UI, macroscopic scoring, and microscopic histopathological examination. The results denoted that the high dose of Ertu (10 mg/kg) demonstrated the most favorable outcomes. Consequently, further biochemical analyses were conducted to elucidate the defensive mechanisms of Ertu opposition to AA-induced UC.

3.4. Effect of high-dose Ertu (10 mg/kg) on biochemical markers

3.4.1. Colonic M1 macrophage biomarkers (CD86, MCP-1, TNF-α, IL-1β and iNOS)

Fig. 4A presents representative immunoblot bands for M1 macrophage biomarkers in colon. As portrayed in Fig. 4B and F, AA provoked inflammatory status and shifted macrophage polarization towards M1-macrophage as witnessed by massive upsurge in the colonic protein

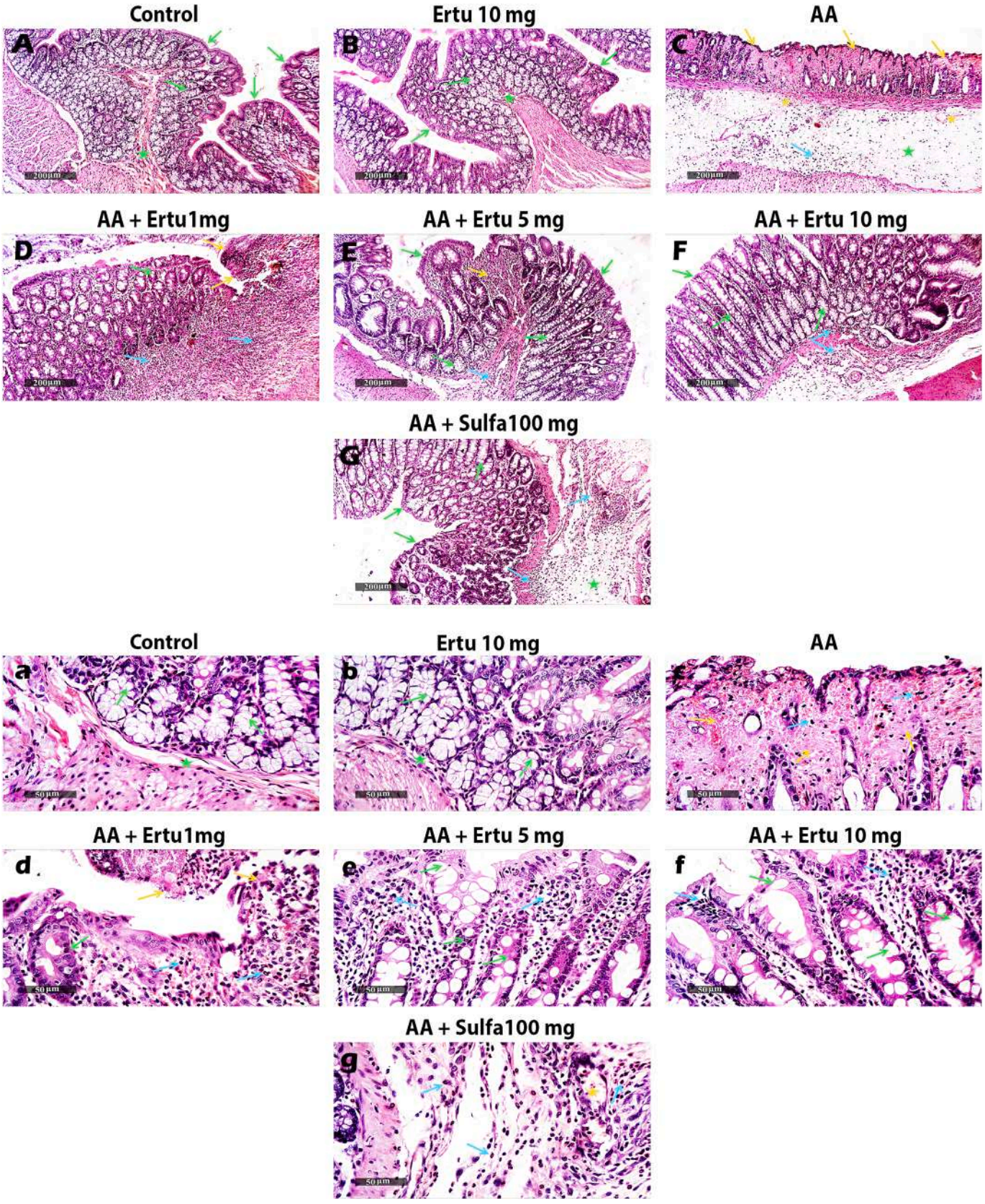

(caption on next page)

Fig. 2. Effect of ertugliflozin (Ertu) (1, 5, and 10 mg/kg) on the histological architecture of rat colon in an AA-induced UC model. Photomicrographs of normal (1 A-a) and drug control (1B-b) groups demonstrated normal colonic walls and intact crypts with abundant goblet cells (green arrow), normal submucosa (green star), and muscular coat. AA group (1C-c) exhibited pronounced ulcerative hemorrhagic colitis and mucosal necrosis (yellow arrow), infiltration of inflammatory cells (blue arrow), vascular congestion (yellow star), and severe submucosal edema (green star). Ertu 1 mg/kg (1D-d) demonstrated persistent mucosal ulceration (yellow arrow), glandular re-epithelialization (green arrow), minimal mature goblet cells, and inflammatory cell infiltrates (blue arrow). Ertu 5 mg/kg (1E-e), 10 mg/kg (1F-f), and Sulfa 100 mg/kg (1G-g) improved colonic wall integrity revealing intact epithelium and mucosal glandular structures, with restored mature goblet cells (green arrow). Ertu 5 mg/kg group showed focal necrosis (yellow arrow) and inflammatory cell aggregates (blue arrow); Ertu 10 mg/kg exhibited reduced inflammatory cells (blue arrow); Sulfa 100 mg/kg had moderate persistence of inflammatory cells (blue arrow), mild vascular congestion (yellow star), and submucosal edema (green star). Panels [A-G]: X100 (scale bar: 200 μm); panels [a-g]: X400 (scale bar: 50 μm). (For interpretation of the references to color in this figure legend, the reader is referred to the web version of this article.)

expressions of CD86 [F (4,10) = 533.3] and MCP-1 [F (4,10) = 189.6] by 6.4- and 4.4-folds-, respectively, as well as the protein contents of TNF-α [F (4,25) = 478.9], IL-1β [F (4,25) = 1678], and iNOS [F (4,25) =1565] by 3.4-, 2.7-, and 4.1-fold, respectively, in comparison to the control group. Conversely, pre-treatment with Ertu (10 mg/kg) as well as Sulfa (100 mg/kg) succeeded in suppressing inflammatory status and reduced the colonic protein expressions of CD86 by 60.2 % and 58.6 %, respectively, MCP-1 by 63.0 % and 60.8 %, respectively, along with the protein contents of TNF-α by 42.1 % and 44.6 %, respectively, IL-1β by 48.8 % and 45.5 %, respectively, and iNOS by 60.8 % and 61.8 %, respectively, relative to AA group. Remarkably, rats pre-treated with Ertu (10 mg/kg) presented a significant drop in the quantity of IL-1β by 6.1 % in comparison to Sulfa pre-treated rats (100 mg/kg).

3.4.2. Colonic M2 macrophage biomarkers (CD206, Fizz-1, Ym-1, Arg-1 and IL-10)

Fig. 5A illustrates representative immunoblot bands for M2 macrophage biomarkers in colon. To further confirm its injurious effect, AA caused a significant drop in colonic M2 macrophage biomarkers, as evidenced by decreases in the protein expressions of CD206 [F (4,10) = 869.9], Fizz-1 [F (4,10) = 433.8], Ym-1 [F (4,10) = 141.8], and Arg-1 [F (4,10) = 1225] along with the protein levels of IL-10 [F (4,25) = 665.8] by 73.4 %, 56.2 %, 64.1 %, 86.6 %, and 59.2 %, respectively, in comparison to the control group **(**Fig. 5B-5F**)**. Contrarily, pre-treatment with Ertu (10 mg/kg) and Sulfa (100 mg/kg) alleviated the inflammation and shifted macrophage polarization towards M2-like macrophage as verified by an elevation in the colonic protein expressions of CD206 by 2.9- and 3.0 folds, respectively, Fizz-1 by 2.1-folds, Ym-1 by 2.3-folds, Arg-1 by 4.8-folds and IL-10 by 2.0-folds as compared to AA group.

3.4.3. Colonic pS536-NF-κB p65, miR-155, claudin-1, occludin, and ZO-1

Fig. 6A presents representative immunoblot bands for NFκB and the tight junction proteins claudin-1, occludin, and ZO-1. As represented in Fig. 6B and F, AA-induced inflammatory status was attributed to an obvious increment in the gene expression of miR-155 [F (4,25) = 581.3] together with the colonic protein expressions of pS635-NF-κB p65 [F (4,10) = 331.6] by 9.6- and 7.6-fold, respectively, relative to the control group. In opposition, administration of Ertu (10 mg/kg) in addition to Sulfa (100 mg/kg) significantly reduced miR-155 gene expression by 55.7 % and 54.5 %, respectively, as well as colonic pS635- NF-κB p65 protein expressions by 53.4 % and 53.1 %, respectively, as compared to AA group.

Similarly, tight junction protein gene expressions; claudin-1 [F (4,25) = 308.8], occludin [F (4,25) = 2384], and ZO-1 [F (4,25) = 7627] **(**Fig. 6C-6E**)** were suppressed in the AA group by 83.1 %, 67.6 %, and 74.5 %, respectively, in comparison to the control group. Meanwhile, pre-treatment with Ertu (10 mg/kg) in addition to Sulfa (100 mg/kg) upregulated claudin-1, occludin, and ZO-1 gene expression by 4-, 2.3-, and 3.2-fold, respectively, as related to AA group.

Correspondingly, tight junction colonic protein expressions; claudin-1 [F (4,25) = 865.7], occludin [F (4,25) = 2823], and ZO-1 [F (4,25) = 4125] **(**Fig. 6G-6I**)** were diminished in the AA group by 76.1 %, 81 %, and 75.8 %, respectively, compared to the control group. In contrast, pre-treatment with Ertu (10 mg/kg) in addition to Sulfa (100 mg/kg) augmented claudin-1, occludin, and ZO-1 protein expression by 3.4-, 4.9-, and 3.4-fold, respectively, as related to AA group.

3.4.4. Colonic oxidative and apoptotic mediators

Apart from its inflammatory effect, AA provoked apoptosis as shown in Fig. 7A-7C and evidenced by a significant increase in the pro-apoptotic protein BAX [F (4,25) = 1359] and BAX/BCL2 ratio [F (4,25) = 1141], which were elevated by 2.3- and 5-fold, respectively. Additionally, there was a 52.1 % reduction in the anti-apoptotic protein BCL2 [F (4,25) = 924.5], in comparison to the control group. However, in contrast, pre-treatment with Ertu (10 mg/kg) and Sulfa (100 mg/kg) inhibited apoptosis as demonstrated by a reduction of BAX protein level by 49.7 % and 49.4 %, respectively, and BAX/ BCL2 ratio by 74.0 %, along with an increase in BCL2 protein level by 1.9-fold as compared to AA group.

Additionally, AA prompted oxidative stress as proven by a significant increase in MDA level, [F (4,25) = 6924], by 2.3-fold in comparison to the control group. Contrariwise, pre-treatment with Ertu (10 mg/kg) in addition to Sulfa (100 mg/kg) succeeded in defeating oxidation and lessened the colonic level of MDA by 48.5 % and 49.5 %, respectively, as compared to AA group **(**Fig. 7D**)**. On the other hand, there was a 58.6 % reduction in the antioxidant SOD level [F (4,25) = 4190] in comparison to the control group. Meanwhile, administration of Ertu (10 mg/kg) as well as Sulfa (100 mg/kg) upregulated SOD level by 2.1-fold as compared to AA group **(**Fig. 7E**)**.

4. Discussion

The present study offered innovative perspectives on the shielding impact of Ertu, an SGLT2 inhibitor, against AA-induced UC in rats, along with the underlying mechanisms contributing to its ameliorative impact. Ertu effectively suppressed the inflammatory transcription factor NF-κB p65 and downregulated the expression of miRNA-155 gene. This led to attenuation of the M1-like macrophage phenotype, as supported by lessened protein expression of CD86 and MCP-1, alongside the protein contents of TNF-α, IL-1β, and iNOS. Simultaneously, Ertu promoted macrophage polarization towards an M2-like phenotype, as witnessed by increased protein expression of CD206, Fizz-1, Ym-1, and Arg-1, along with elevated IL-10 protein content. Moreover, Ertu enhanced the tight junction protein gene expressions, including claudin-1, occludin, and ZO-1, aiding in the restoration of intestinal epithelial integrity. Additionally, Ertu moderated oxidative stress by significantly decreasing MDA, the lipid peroxidation indicator, and enhancing the levels of antioxidant SOD. Finally, Ertu mitigated apoptosis by decreasing the apoptotic protein BAX and enhancing the anti-apoptotic protein, BCL2 content. These newly discovered findings reinforce earlier research on SGLT2 inhibitors, highlighting a noteworthy association between SGLT2 inhibitors and UC and confirming their potential protective effects. The protective benefits of gliflozins have previously been demonstrated in studies with canagliflozin [24,56], dapagliflozin [23,57] and empagliflozin in UC rat models [3,21].

In the current study, intra-rectal administration of AA initiated significant histological, macroscopic, and microscopic damage to the rat colon, consistent with previous studies [37,58]. These alterations included mucosal hemorrhagic ulcerative lesions, necrosis, abscess formation, submucosal inflammatory cell infiltration, and marked edema.

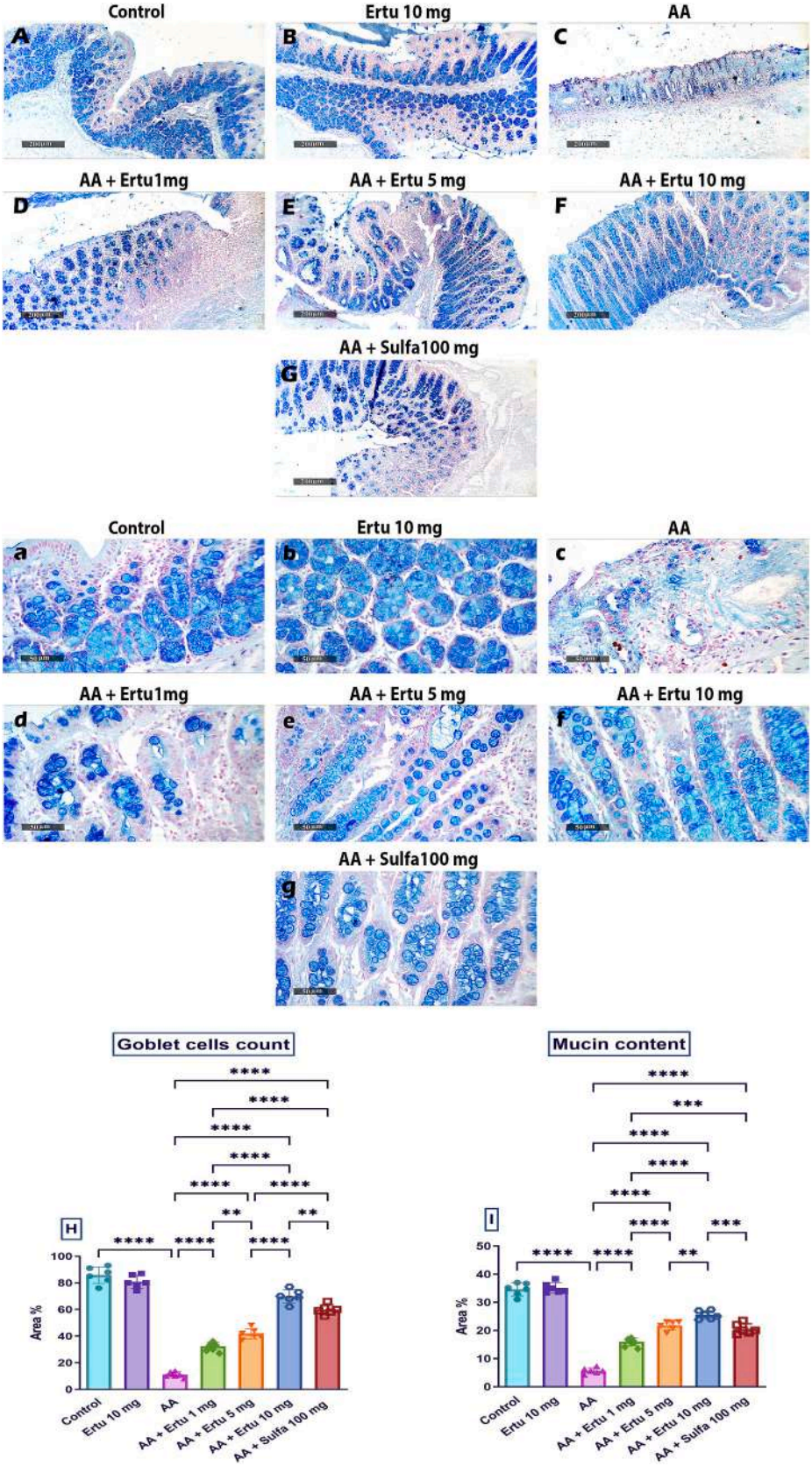

(caption on next page)

Fig. 3. Effect of ertugliflozin (Ertu) (1, 5, and 10 mg/kg) on mucosal goblet cell counts and acidic mucin content in colonic tissues stained with Alcian blue (pH 2.5). Photomicrographs represented the following groups: (A, a) Control, (B, b) Drug control, (C, c) AA, (D, d) AA + Ertu 1 mg/kg, (E, e) AA + Ertu 5 mg/kg, (F, f) AA + Ertu 10 mg/kg, and (G, g) AA + Sulfa. Panels [A-G]: X100 (scale bar: 200 μm); panels [a-g]: X400 (scale bar: 50 μm). Panel (H) illustrates the area percentage of goblet cell count and panel (I) presents the area percentage of acidic mucin content. Data are depicted as mean ± SD ($n = 6$ per group). Statistical evaluation was conducted via one-way ANOVA succeeded by Tukey's post hoc test; ** $p < 0.01$, *** $p < 0.001$ and **** $p < 0.0001$. (For interpretation of the references to color in this figure legend, the reader is referred to the web version of this article.)

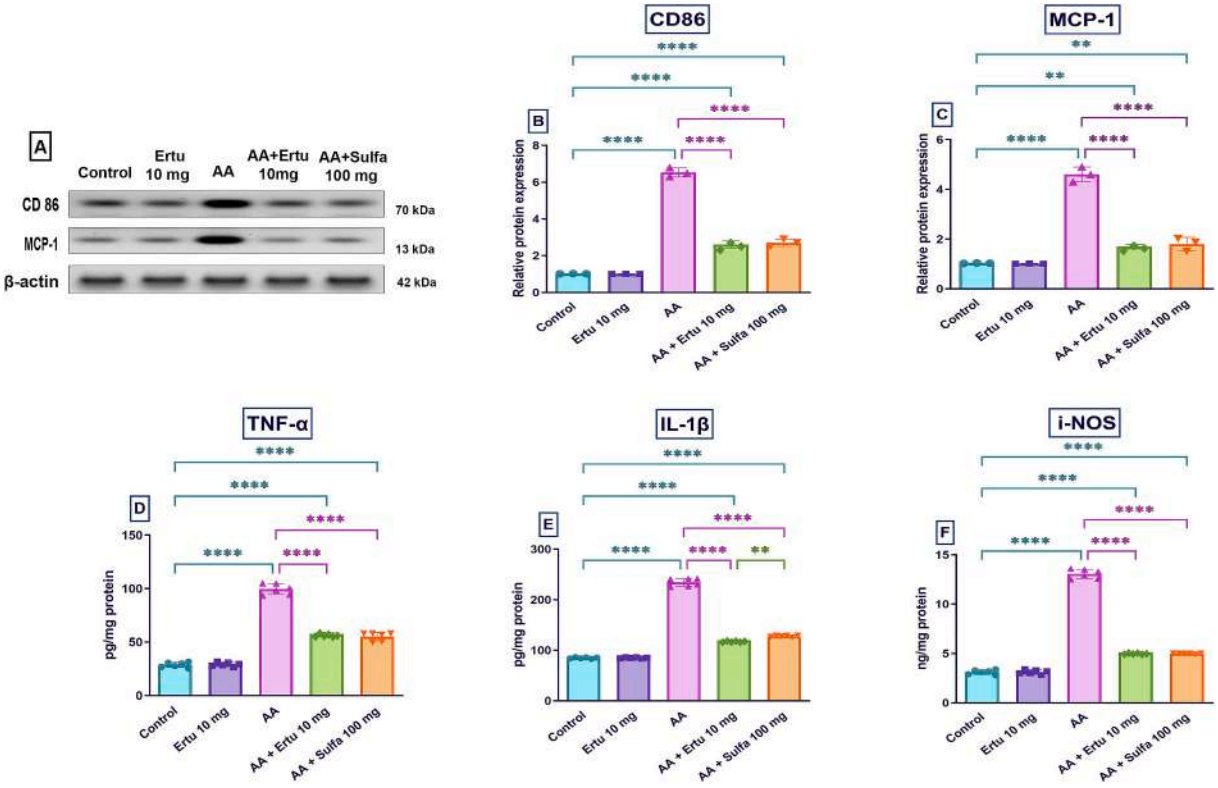

Fig. 4. The effect of Ertu (10 mg/kg) on colonic protein expression and levels of M1 macrophage markers in an AA-induced UC rat model. (A) Representative Western blot bands for CD86 and MCP-1. (B) Quantification of CD86 protein expression. (C) Quantification of MCP-1 protein expression. Protein contents of (D) TNF-α, (E) IL-1β, and (F) iNOS. Data are depicted as mean ± SD ($n = 3$ per group for WB and n = 6 for ELISA). Statistical evaluation was conducted via one-way ANOVA succeeded by Tukey's post hoc test; ** $p < 0.01$ and **** $p < 0.0001$. AA, acetic acid; CD86, cluster of differentiation 86; Ertu, ertugliflozin; iNOS, inducible nitric oxide synthase; IL-1β, interleukin-1 beta; MCP-1, monocyte chemoattractant protein-1; Sulfa, sulfasalazine; TNF-α, tumor necrosis factor-alpha.

This damage disrupted the mucus layer, leading to goblet cell loss and reduced mucin content, thereby compromising the intestinal barrier. Furthermore, AA-treated rats exhibited pronounced macroscopic damage, characterized by increased DAI [37,44], colon mass index [46], the ratio of colon weight to length [40,47], UI [44], and colonic damage score [49,50]. Conversely, pre-treatment with Ertu alleviated AA-induced UC in rats, as demonstrated by improvements in both the histological architecture of the colon and macroscopic evaluations, which assessed the severity of intestinal inflammation. These therapeutic upshots were observed following a dose-dependent way, with the high dose of Ertu (10 mg/kg/day, p.o.) demonstrating particularly significant biochemical outcomes. Furthermore, the therapeutic efficacy of Ertu was comparable to Sulfa, which served as the reference drug for evaluating its effectiveness against UC.

The pathophysiology of UC is characterized by a dysregulated immune response that overreacts to normal gut microbiota, leading to chronic inflammation [59]. Macrophages, as essential innate immune cells, engage in a principal function in the pathogenesis of UC [60]. Macrophages can undergo polarization into two distinct phenotypes: M1 (proinflammatory) and M2 (anti-inflammatory). M1 macrophages produce excessive pro-inflammatory cytokines, which lead to barrier damage and inflammation, meanwhile, M2 macrophages promote tissue regeneration and wound healing [61]. Macrophages, particularly those of the M2 phenotype, enhance intestinal epithelial tight-junction integrity through exosomes delivery of microRNAs (e.g., miR-590-3p, miR-21 and miR-23a-3p) that promote epithelial proliferation and repair, as well as cytokine secretion, notably transforming growth factor beta, which upregulates key tight-junction proteins such as claudin-1, claudin-4, and occludin, thereby maintaining barrier function [62,63].

Noteworthy, the NF-κB signaling pathway serves a crucial function in driving the classical stimulation of M1 macrophages [64]. Upon activation, IκBα undergoes phosphorylation, ubiquitination, and subsequent degradation in the cytoplasm. This degradation allows the relocation of NF-κB to the nucleus, in which it stimulates pro-inflammatory indicators production as TNF-α, IL-1β, MCP-1, and iNOS as reported herein and previously [60,61,65]. This cascade amplified the inflammatory response, facilitated M1 macrophage activation, and increased the protein expression of CD86, a key marker for M1 macrophages. Conversely, NF-κB activation inhibited M2 macrophage polarization as witnessed in the reduction of the protein expression of Arg-1, Fizz-1, and Ym-1, along with IL-10 protein level. This suppression also led to a decline in CD206 expression, a characteristic marker of M2 macrophages [66,67]. Therefore, restoring the balance between M1 and M2 macrophages holds significant potential for the treatment of UC, making macrophage polarization a promising therapeutic target.

The present research, for the first time, demonstrated that Ertu

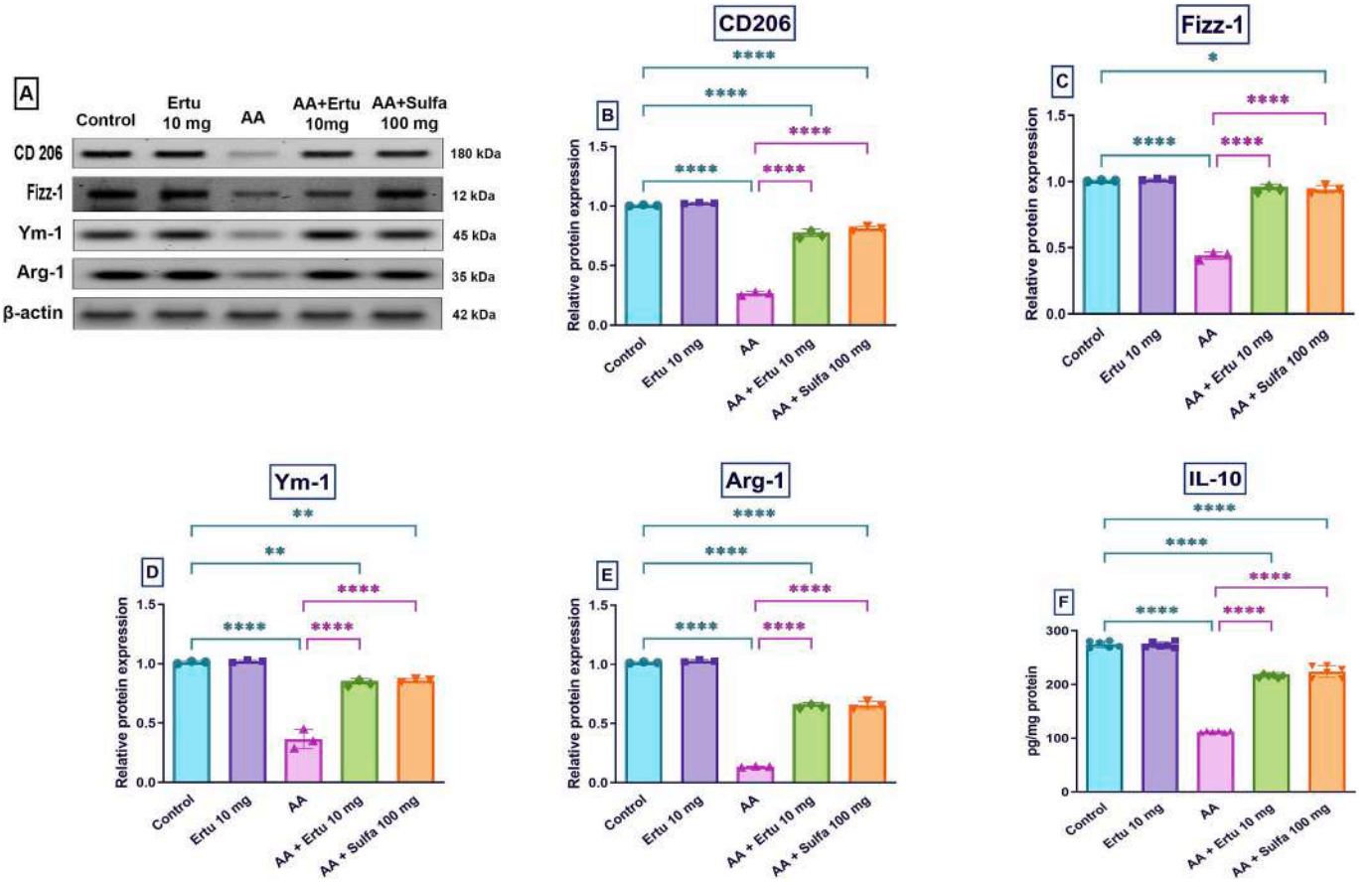

Fig. 5. The effect of Ertu (10 mg/kg) on colonic protein expression and levels of M2 macrophage markers in AA-induced UC rat model. (A) Representative Western blot bands for CD206, Fizz-1, Ym-1, and Arg-1. Quantification of protein expression levels for (B) CD206, (C) Fizz-1, (D) Ym-1, (E) Arg-1, and (F) IL-10 protein content. Data are depicted as mean ± SD (n = 3 per group for WB and n = 6 for ELISA). Statistical evaluation was conducted via one-way ANOVA succeeded by Tukey's post hoc test; * $p < 0.05$, ** $p < 0.01$ and **** $p < 0.0001$. AA, acetic acid; Arg-1, arginase-1; CD206, cluster of differentiation 206; Ertu, ertugliflozin; Fizz-1, found in inflammatory zone-1; IL-10, interleukin-10; Ym-1, chitinase-3-like protein 1; Sulfa, sulfasalazine.

attenuated the inflammatory status and shifted macrophage polarization towards the M2 phenotype via inhibiting the NF-κB signaling pathway. Indeed, pre-treatment with Ertu attenuated M1 macrophages activation and decreased the secretion of its pro-inflammatory cytokine, such as TNF-α, IL-1β, MCP-1, iNOS, and CD86, thereby alleviating AA-induced inflammation in the colon of the rats. Simultaneously, Ertu promoted the polarization of M2 macrophages, increasing the protein expression of Arg-1, Fizz-1, Ym-1, and CD206 together with IL-10 levels, which contributed to tissue repair and regeneration. Also, the anti-inflammatory upshots of Ertu can be supported by the study of Moellmann et al. [32] which demonstrated that Ertu triggered the phosphorylation of cardiac AMP-activated protein kinase (AMPK) at Thr172, thereby influencing M1/M2 macrophage polarization. Similarly, Ertu significantly reduced p-AKT (Ser473), p-AKT (Thr308), and IL-1β, suggesting that Ertu effectively modulates M1/M2 polarization. These previous findings suggest that the phosphatidylinositol-3-kinase /Akt/NF-κB signaling axis plays a role in inhibiting M1 macrophage polarization [68]. In the bargain, earlier studies have highlighted Ertu's anti-inflammatory effects, including the downregulation of key inflammatory mediators for instance NF-κB, IL-1β, IL-6, TNF-α, toll-like receptor 4 (TLR4), and macrophage migration inhibitory factor [69,70].

Notably, several studies have underlined the significance of M1/M2 polarization in UC. Ge et al. [65] reported that isomeranzin improved experimentally induced colitis by modulating M1 macrophage polarization through the NF-κB and ERK pathways. Similarly, Min-yao et al. [71] showed that Huangqin decoction alleviated UC by influencing fatty acid metabolism, which in turn regulates M2 macrophage polarization via the FFAR4-AMPK-PPARα pathway. Additionally, Hongda et al. [15] demonstrated that tiliroside mitigated UC by restoring the balance between M1 and M2 macrophages. It has been well-established that the administration of empagliflozin, another SGLT2 inhibitor, leads to a reduction in M1 macrophage polarization while promoting the activation of the alternative M2 macrophages, thereby protecting against excessive inflammation [72]. Previous studies have also suggested that SGLT2 inhibitors, including dapagliflozin, exhibited anti-inflammatory and antioxidant effects. Dapagliflozin was shown to induce a shift from the M1 macrophage phenotype, characterized by markers for instance IL-6, IL-1β, and iNOS, towards the M2 phenotype, represented by markers such as CD206 and IL-10. This shift occurred through the activation of the STAT3 signaling pathway, ultimately attenuating cardiac fibrosis [73]. Furthermore, canagliflozin has demonstrated anti-inflammatory and neuroprotective properties by hindering the TLR4/MyD88/NF-κB/NLRP3 pathway, which resulted in modulation of the M1 to M2 phenotypic shift in microglial polarization, thereby reducing apoptosis and inflammation [55].

Of note, miR-155 has been linked to various inflammatory responses and was stated to be over-expressed in UC [74,75]. In UC, the amplification of miR-155 enhances NF-κB activity, which consequently amplifies the production of mediators of inflammation, exacerbating inflammation [75]. Additionally, the overexpression of miR-155 leads to the downregulation of TJ proteins, disrupting the intestinal mucosal barrier [76]. MiR-155 has also been shown to be involved in the polarization of macrophages, contributing to inflammation. There is substantial evidence indicating that TLR4/MyD88 signaling plays a critical

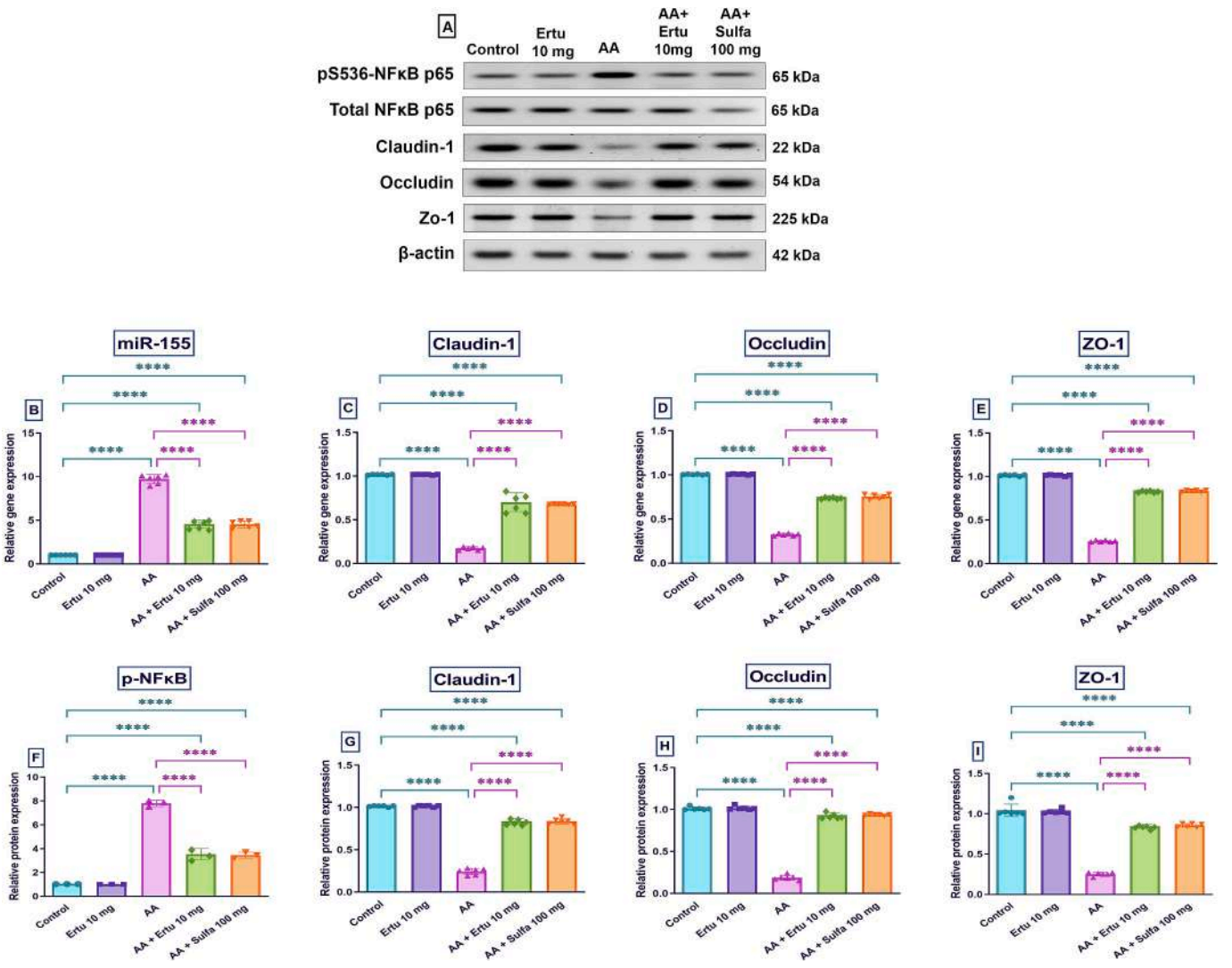

Fig. 6. The effect of Ertu (10 mg/kg) on colonic protein and gene expression of inflammatory and tight junction markers in AA-induced UC rat model. (A) Representative Western blot bands for pS536-, total NF-κB p65, claudin-1, occludin, and ZO-1. Gene expression levels of (B) miR-155, (C) claudin-1, (D) occludin, and (E) ZO-1. Quantification of (F) pS635-NF-κB, (G) claudin-1, (H) occludin, and (I) ZO-1 protein expression. Data are depicted as mean ± SD (n = 3 per group for WB and n = 6 for PCR). Statistical evaluation was conducted via one-way ANOVA succeeded by Tukey's post hoc test; **** $p < 0.0001$. AA, acetic acid; Ertu, ertugliflozin; miR-155, microRNA 155; pS536-NFκB p65, phospho-serine 536 nuclear factor-kappa B; Sulfa, sulfasalazine; ZO-1, zonula occludens-1.

role in regulating miR-155 expression. Upstream miR-155 induced expression is likely regulated by the TLR4/MyD88/NF-κB pathway, a well-characterized inflammatory signaling axis known to induce miR-155 in macrophages and epithelial cells [77,78]. Therefore, targeting miR-155 inhibition presents a promising therapeutic approach for managing UC. Indeed, inhibiting miR-155 was shown to reduce p-NF-κB activation and lower inflammatory cytokine release, alleviating colitis severity [76,79]. Research indicates that miR-155 is critical in regulating macrophage polarization during colitis. Specifically, down-regulating miR-155 expression leads to a shift from the pro-inflammatory M1 macrophage phenotype to the anti-inflammatory M2 phenotype, helping to suppress inflammation and modulate adaptive immune responses in the colon [80]. These findings align with the current study, where treatment with Ertu significantly reduced miR-155 expression, contributing to its anti-inflammatory effects. This outcome is further supported by studies showing that SGLT2 inhibitors, such as dapagliflozin, reduced miR-155 expression, promoting a shift towards M2 macrophage polarization via NF-κB pathway inhibition [81,82].

Tight junction proteins, such as claudin-1, occludin, and ZO-1 have a critical function in conserving gut barrier integrity by binding intestinal epithelial cells together [83]. During the progression of UC, disruption of TJ leads to compromised gut barrier function, increased intestinal permeability, microbial translocation, and persistent inflammation [84,85]. Thus, preserving TJ function is essential for preventing the invasion of enteric pathogens and other harmful substances within the intestinal mucosa, thereby mitigating immune responses.

In the current study, AA administration reduced the gene expression of claudin-1, occludin, and ZO-1, thereby impairing the integrity of the colonic membrane. These findings align with previous studies [83,86]. Conversely, pre-treatment with Ertu significantly elevated the expression of these TJ proteins, which may explain its colo-protective effects. This upregulation could result from the inhibition of the NF-κB signaling cascade and its associated inflammatory cascade. These observations are in line with the studies of Lei et al. [87] and Duo-duo et al. [85], which demonstrated that increased TJ protein expression alleviates UC symptoms by restoring intestinal mucosal integrity through the suppression of NF-κB pathway. Similarly, empagliflozin, an SGLT2 inhibitor, has remarkably boosted the contents of TJ proteins; claudin-1 and occludin, thereby improving colonic barrier function and promoting mucosal healing via NF-κB pathway inhibition [3].

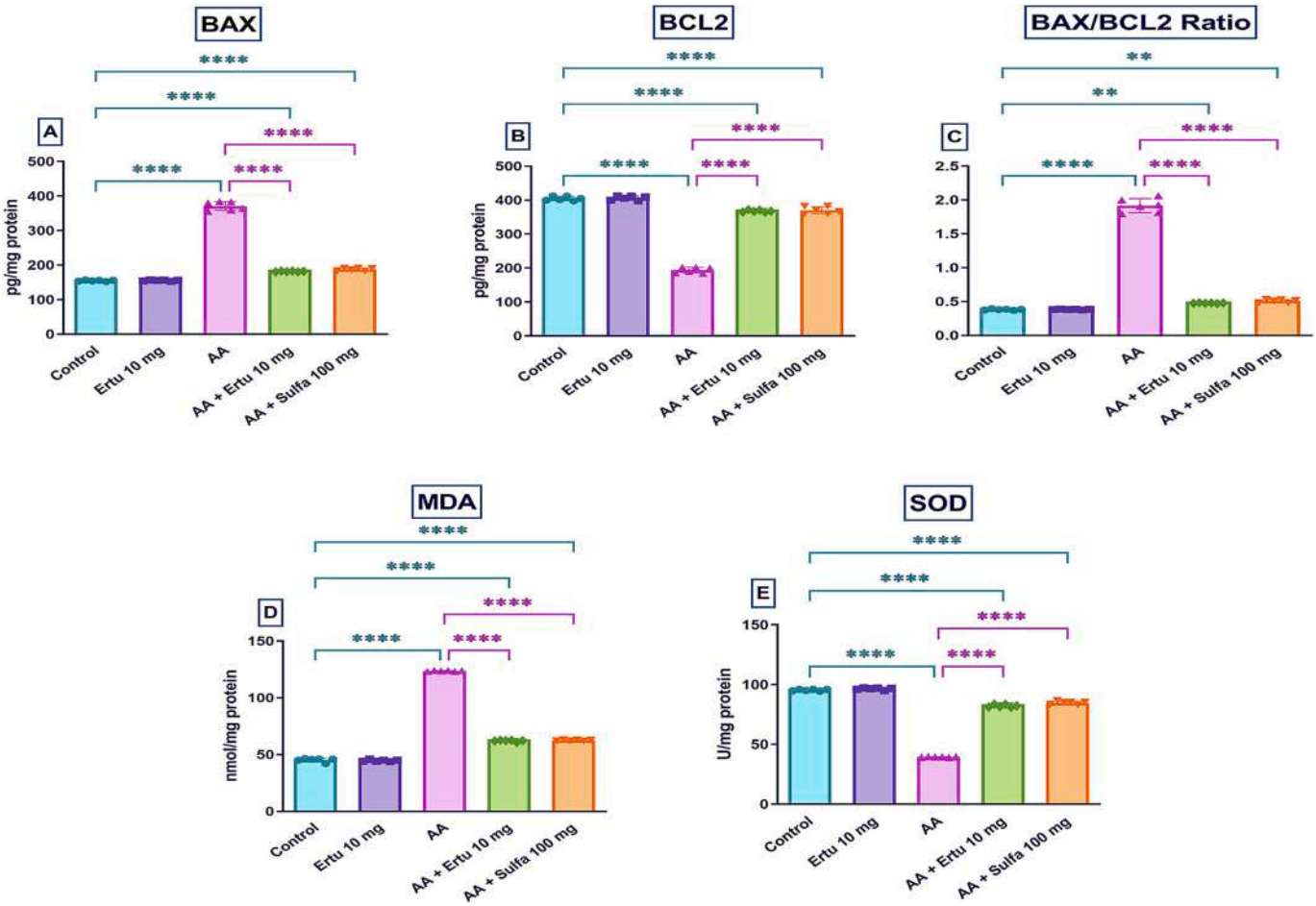

Fig. 7. The effect of Ertu (10 mg/kg) on colonic protein levels of (A) BAX, (B) BCL2, (C) BAX/ BCL2 ratio, (D) MDA and (E) SOD in an AA-induced UC rat model. Data are depicted as mean ± SD (n = 6 per group), Statistical evaluation was conducted via one-way ANOVA succeeded by Tukey's post hoc test; ** $p < 0.01$ and **** $p < 0.0001$. AA, acetic acid; BAX, BCL2-Associated X Protein; BCL2, B-cell lymphoma protein 2; Ertu, ertugliflozin; MDA, malondialdehyde; SOD, superoxide dismutase; Sulfa, sulfasalazine.

Oxidative stress plays a vital role in maintaining normal cellular functions at physiological levels; however, when excessively activated, it can exacerbate intestinal barrier disruption and promote epithelial cell death. Moreover, it has been implicated as a key contributor to the pathogenesis of ulcerative colitis [88]. MDA is a major byproduct of lipid peroxidation, resulting from the reaction between oxygen free radicals and unsaturated fatty acids in cell membranes. It exerts considerable harmful effects on the colonic mucosa. Therefore, MDA is widely used as an indirect marker to assess oxygen free radical's levels in the colonic tissue of patients with UC. Besides, SOD plays a crucial role in neutralizing oxygen free radicals, preventing lipid peroxidation within intestinal tissues, and maintaining the stability of cell membranes. As a result, SOD is widely regarded as a key indicator of the body's antioxidant defense capacity against oxidative stress [89,90]. Based on these findings, the current study showed AA administration led to an upregulation of MDA levels, alongside a reduction in SOD content, which is consistent with earlier studies [91,92]. Conversely, pretreatment with Ertu suppressed oxidative stress by lowering the levels of MDA while enhancing SOD content. These findings are in line with earlier research [93] which confirmed that Ertu exhibited oxidative stress-inhibiting properties.

The apoptotic pathway plays a crucial role in UC pathogenesis, adjusted by the equilibrium amid the pro-apoptotic proteins (e.g., BAX) and anti-apoptotic proteins (e.g., BCL2). An elevated BAX/BCL2 ratio activates caspase-3, enhancing apoptosis [94]. Intestinal epithelial cells are essential for maintaining immune responses, mucosal homeostasis, and host defense. However, apoptosis triggered via the TLR4/NF-κB axis disrupts the epithelial barrier, leading to intestinal injury, improper fluid secretion, and symptoms such as diarrhea, gas, and cramping. Thus, restoring mucosal barrier integrity by inhibiting apoptosis improves UC outcomes [95,96]. In light of these outcomes, the present study demonstrated that AA administration raised BAX and caspase-3 levels while reducing BCL2 levels, aligning with previous research [94,97]. On the other hand, pre-treatment with Ertu inhibited apoptosis by reducing BAX and caspase-3 and increasing BCL2 content, an effect likely correlated with the repression of the NF-κB signaling pathway. This was consistent with previous studies [32,34], which demonstrated that Ertu exerted anti-apoptotic effects by repressing BAX and caspase-3 while boosting BCL2. Similarly, canagliflozin, an SGLT2 inhibitor, has been shown to reduce the BAX/BCL2 ratio and caspase-3 levels in UC models [24,56]. Furthermore, the anti-apoptotic effects of dapagliflozin in UC have been attributed to its ability to suppress caspase-3 expression [23].

Regarding the comparison between the high dose of Ertu (10 mg/kg) and the standard drug Sulfa in alleviating AA-induced UC, both exhibited nearly the same results including the histological, macroscopic, and biochemical assay markers in light of the previous literature which unveiled the robust effect of Sulfa in the treatment of UC [98].

In conclusion, Ertu alleviated AA-induced UC in rats by inhibiting the NF-κB signaling cascade and its downstream pro-inflammatory cytokines, thereby promoting a shift in macrophage polarization from the pro-inflammatory M1 phenotype to the anti-inflammatory M2

phenotype. Additionally, Ertu suppressed the expression of miR-155, restored mucosal barrier integrity by upregulating the TJ proteins, and mitigated apoptosis and oxidative stress. These findings position Ertu as another promising SGLT2 inhibitor with protective effects against UC, paving the way for future research into its therapeutic potential in other inflammatory bowel diseases.

The present study has some limitations that warrant future consideration. To comprehensively evaluate the therapeutic efficacy of Ertu in UC, its impact should be examined across different experimental models in addition to AA, including chronic models, such as DSS or TNBS, which would allow a more thorough evaluation of the long-term impact of Ertu on disease progression and mucosal healing, as well as genetically modified models that better mimic human disease pathogenesis. Also, future research needs to evaluate the safety and efficacy of co-administering Ertu with anti-TNF-α biologics utilized in UC treatment. Direct quantification of infiltrating macrophages as CD68+/CD163+ cells could complement the current findings as well as, directly assessing M1/M2 polarization markers in macrophages themselves rather than detecting them in rat tissues. Assessment of BAX and BCL2 expression using Western blotting or the TUNEL assay could further validate the results by providing advanced apoptosis detection data. Future research should also include direct measurements of blood or urine volume, osmolality, and hematocrit to conclusively rule out adverse effects of Ertu as an osmotic diuretic.

CRediT authorship contribution statement

Marina R. Fouad: Writing – review & editing, Writing – original draft, Visualization, Validation, Supervision, Software, Resources, Project administration, Methodology, Investigation, Funding acquisition, Formal analysis, Data curation, Conceptualization. **Mostafa A. Rabie:** Writing – review & editing, Visualization, Validation, Supervision, Resources, Investigation, Formal analysis, Data curation, Conceptualization. **Hala F. Zaki:** Writing – review & editing, Visualization, Validation, Supervision, Investigation, Formal analysis, Data curation, Conceptualization. **Rania M. Salama:** Writing – review & editing, Visualization, Validation, Supervision, Resources, Methodology, Investigation, Formal analysis, Data curation, Conceptualization.

Funding

There was no specific grant awarded for this study by public, commercial or nonprofit funding organizations.

Declaration of competing interest

The authors declare that they have no known competing financial interests or personal relationships that could have appeared to influence the work reported in this paper.

Data availability

Data will be made available on request.

References

[1] H.M. Hafez, M.A. Ibrahim, W. Yehia Abdelzaher, A.A. Gad, S. Mohammed Naguib Abdel Hafez, S.A. Abdel-Gaber, Protective effect of mirtazapine against acetic acid-induced ulcerative colitis in rats: role of NLRP3 inflammasome pathway, Int. Immunopharmacol. 101 (Pt A) (2021) 108174, https://doi.org/10.1016/j.intimp.2021.108174.

[2] W. Wei, L. Wang, K. Zhou, H. Xie, M. Zhang, C. Zhang, Rhapontin ameliorates colonic epithelial dysfunction in experimental colitis through SIRT1 signaling, Int. Immunopharmacol. 42 (2017) 185–194, https://doi.org/10.1016/j.intimp.2016.11.024.

[3] M.S. Zaghloul, M. Elshal, M.E. Abdelmageed, Preventive empagliflozin activity on acute acetic acid-induced ulcerative colitis in rats via modulation of SIRT-1/PI3K/AKT pathway and improving colon barrier, Environ. Toxicol. Pharmacol. 91 (2022) 103833, https://doi.org/10.1016/j.etap.2022.103833.

[4] M. Gajendran, P. Loganathan, G. Jimenez, A.P. Catinella, N. Ng, C. Umapathy, N. Ziade, J.G. Hashash, A comprehensive review and update on ulcerative colitis, Disease-a-Month 65 (12) (2019) 100851, https://doi.org/10.1016/j.disamonth.2019.02.004.

[5] J.O. Dawood, A. Abu-Raghif, Labetalol ameliorates experimental colitis in rat possibly through its effect on Proinflammatory mediators and oxidative stress, Clin. Lab. 70 (2) (2024), https://doi.org/10.7754/Clin.Lab.2023.230659.

[6] A.A. Abdelsameea, A.E. Alsemeh, N. Alabassery, W. Samy, A. Fawzy, N.A.T. Abbas, Icosapent ethyl alleviates acetic acid-induced ulcerative colitis via modulation of SIRT1 signaling pathway in rats, Int. Immunopharmacol. 115 (2023) 109621, https://doi.org/10.1016/j.intimp.2022.109621.

[7] K. Wang, Y.-f. Li, Q. Lv, X.-m. Li, Y. Dai, Z.-f. Wei, Bergenin, acting as an agonist of PPARγ, ameliorates experimental colitis in mice through improving expression of SIRT1, and therefore inhibiting NF-κB-mediated macrophage activation, Front. Pharmacol. 8 (2018) 981.doi:https://doi.org/10.3389/fphar.2017.00981.

[8] F.N. Shahraki, S. Momtaz, M. Baeeri, D. Khayatan, N.A. Lashgari, N.M. Roudsari, A. R. Abdollahi, A.R. Dehpour, A.H. Abdolghaffari, Licofelone attenuates acetic acid-induced colitis in rats through suppression of the inflammatory mediators, Inflammation 46 (5) (2023) 1709–1724, https://doi.org/10.1007/s10753-023-01835-0.

[9] M. Ghasemi-Dehnoo, H. Amini-Khoei, Z. Lorigooini, K. Ashrafi-Dehkordi, M. Rafieian-Kopaei, Coumaric acid ameliorates experimental colitis in rats through attenuation of oxidative stress, inflammatory response and apoptosis, Inflammopharmacology 30 (6) (2022) 2359–2371, https://doi.org/10.1007/s10787-022-01074-z.

[10] M.A. Oraby, S.S. Abdel Mageed, A. Amr Raouf, D.A. Abdelshafy, E.F. Ahmed, R. T. Khalil, S.A. Mangoura, D.S. Fadaly, Remdesivir ameliorates ulcerative colitis-propelled cell inflammation and pyroptosis in acetic acid rats by restoring SIRT6/FoxC1 pathway, Int. Immunopharmacol. 137 (2024) 112465, https://doi.org/10.1016/j.intimp.2024.112465.

[11] M. Kawada, A. Arihiro, E. Mizoguchi, Insights from advances in research of chemically induced experimental models of human inflammatory bowel disease, World J. Gastroenterol. 13 (42) (2007) 5581–5593, https://doi.org/10.3748/wjg.v13.i42.5581.

[12] R. Patra, S. Padma, S. Mukherjee, An improved method for experimental induction of ulcerative colitis in Sprague Dawley rats, MethodsX 10 (2023) 102158, https://doi.org/10.1016/j.mex.2023.102158.

[13] J. Wang, C. Zhang, C. Guo, X. Li, Chitosan ameliorates DSS-induced ulcerative colitis mice by enhancing intestinal barrier function and improving microflora, Int. J. Mol. Sci. 20 (22) (2019) 5751, https://doi.org/10.3390/ijms20225751.

[14] S. Pasca, A. Jurj, B. Petrushev, C. Tomuleasa, D. Matei, MicroRNA-155 implication in M1 polarization and the impact in inflammatory diseases, Front. Immunol. 11 (2020) 625, https://doi.org/10.3389/fimmu.2020.00625.

[15] H. Zhuang, Q. Lv, C. Zhong, Y. Cui, L. He, C. Zhang, J. Yu, Tiliroside ameliorates ulcerative colitis by restoring the M1/M2 macrophage balance via the HIF-1α/glycolysis pathway, Front. Immunol. 12 (2021), https://doi.org/10.3389/fimmu.2021.649463.

[16] J. Zheng, S. Wang, T. Zhang, H. Li, M. Zhu, X. Wei, Y. Ge, X. Yang, S. Zhang, H. Xu, Y. Duan, L. Liu, Y. Chen, Nogo-B inhibition restricts ulcerative colitis via inhibiting p68/miR-155 signaling pathway, Int. Immunopharmacol. 120 (2023) 110378, https://doi.org/10.1016/j.intimp.2023.110378.

[17] A. Yousefi-Ahmadipour, A. Rashidian, M.R. Mirzaei, A. Farsinejad, F. PourMohammadi-Nejad, M. Ghazi-Khansari, J. Ai, S. Shirian, A. Allahverdi, J. Saremi, S. Ebrahimi-Barough, Combination therapy of mesenchymal stromal cells and sulfasalazine attenuates trinitrobenzene sulfonic acid induced colitis in the rat: the S1P pathway, J. Cell. Physiol. 234 (7) (2019) 11078–11091, https://doi.org/10.1002/jcp.27944.

[18] N. Aslam, S.W. Lo, R. Sikafi, T. Barnes, J. Segal, P.J. Smith, J.K. Limdi, A review of the therapeutic management of ulcerative colitis, Therap. Adv. Gastroenterol. 15 (2022) 17562848221138160, https://doi.org/10.1177/17562848221138160.

[19] E.N. Oubaid, A. Abu-Raghif, I.M. Al-Sudani, Ibudilast ameliorates experimentally induced colitis in rats via down-regulation of proinflammatory cytokines and myeloperoxidase enzyme activity, Pharmacia 70 (2023) 187–195, https://doi.org/10.3897/pharmacia.70.e98715.

[20] M.J. Manna, A. Abu-Raghif, O. Al-Saree, The value of doxycycline in acetic acid induce ulcerative colitis in rats, Int. J. Pharm. Sci. Res. 9 (8) (2018) 3567–3572, https://doi.org/10.13040/IJPSR.0975-8232.9(8).3567-72.

[21] A. Makaro, M. Swierczynski, K. Pokora, B. Sarniak, R. Kordek, J. Fichna, M. Salaga, Empagliflozin attenuates intestinal inflammation through suppression of nitric oxide synthesis and myeloperoxidase activity in in vitro and in vivo models of colitis, Inflammopharmacology 32 (1) (2024) 377–392, https://doi.org/10.1007/s10787-023-01227-8.

[22] M.E. Youssef, E.E. Abd El-Fattah, A.M. Abdelhamid, H. Eissa, E. El-Ahwany, N. A. Amin, H.F. Hetta, M.H. Mahmoud, G.E. Batiha, N. Gobba, A.G. Ahmed Gaafar, S. Saber, Interference with the AMPKalpha/mTOR/NLRP3 signaling and the IL-23/IL-17 Axis effectively protects against the dextran sulfate sodium intoxication in rats: a new paradigm in Empagliflozin and metformin Reprofiling for the Management of Ulcerative Colitis, Front. Pharmacol. 12 (2021) 719984, https://doi.org/10.3389/fphar.2021.719984.

[23] M.K. ElMahdy, S.A. Antar, E.K. Elmahallawy, W. Abdo, H.H.A. Hijazy, A. Albrakati, A.E. Khodir, A novel role of Dapagliflozin in mitigation of acetic acid-induced ulcerative colitis by modulation of monocyte chemoattractant protein 1 (MCP-1)/nuclear factor-kappa B (NF-kappaB)/Interleukin-18 (IL-18), Biomedicines 10 (1) (2021), https://doi.org/10.3390/biomedicines10010040.

[24] M.A. Morsy, H.M. Khalaf, R.A. Rifaai, A.M.A. Bayoumi, E. Khalifa, Y.F. Ibrahim, Canagliflozin, an SGLT-2 inhibitor, ameliorates acetic acid-induced colitis in rats

through targeting glucose metabolism and inhibiting NOX2, Biomed. Pharmacother. 141 (2021) 111902, https://doi.org/10.1016/j.biopha.2021.111902.
[25] A.H. Abbas, Z.H. Abbas, H.R. Salman, H.E. Jabar, A.H. Abd, The attenuated effects of topical empagliflozin on imiquimod-induced model of psoriasis in mice: the attenuated effects of topical empagliflozin on imiquimod-induced model of psoriasis in mice, J. Trop. Life Sci. 14 (3) (2024) 459–468, https://doi.org/10.11594/jtls.14.03.03.
[26] H. Ridha-Salman, A.A. Al-Zubaidy, A.H. Abbas, D.M. Hassan, S.A. Malik, The alleviative effects of canagliflozin on imiquimod-induced mouse model of psoriasis-like inflammation, Naunyn Schmiedebergs Arch. Pharmacol. 398 (3) (2025) 2695–2715, https://doi.org/10.1007/s00210-024-03406-y.
[27] H. Hanaoka, J. Kikuchi, K. Hiramoto, M. Akiyama, S. Saito, Y. Kondo, T. Azegami, Y. Kaneko, Dapagliflozin for rheumatic musculoskeletal disease in patients with chronic kidney disease, Mod. Rheumatol. 35 (2) (2024) 345–351, https://doi.org/10.1093/mr/roae090.
[28] H. Lu, H. Lu, C. Kosinski, A. Wojtusciszyn, A. Zanchi, P.N. Carron, M. Müller, P. Meyer, J. Martin, O. Muller, R. Hullin, SGLT2 inhibitors, what the emergency physician needs to know: a narrative review, J. Clin. Med. 10 (9) (2021), https://doi.org/10.3390/jcm10092036.
[29] D.J. Fediuk, G. Nucci, V.K. Dawra, D.L. Cutler, N.B. Amin, S.G. Terra, R.A. Boyd, R. Krishna, V. Sahasrabudhe, Overview of the clinical pharmacology of Ertugliflozin, a novel sodium-glucose cotransporter 2 (SGLT2) inhibitor, Clin. Pharmacokinet. 59 (8) (2020) 949–965, https://doi.org/10.1007/s40262-020-00875-1.
[30] X. Qiu, S. Xie, L. Ye, R.A. Xu, UPLC-MS/MS method for the quantification of ertugliflozin and sitagliptin in rat plasma, Anal. Biochem. 567 (2019) 112–116, https://doi.org/10.1016/j.ab.2018.12.016.
[31] S.G. Terra, K. Focht, M. Davies, J. Frias, G. Derosa, A. Darekar, G. Golm, J. Johnson, D. Saur, B. Lauring, S. Dagogo-Jack, Phase III, efficacy and safety study of ertugliflozin monotherapy in people with type 2 diabetes mellitus inadequately controlled with diet and exercise alone, Diabetes Obes. Metab. 19 (5) (2017) 721–728, https://doi.org/10.1111/dom.12888.
[32] J. Moellmann, P.A. Mann, B.A. Kappel, F. Kahles, B.M. Klinkhammer, P. Boor, R. Kramann, B. Ghesquiere, C. Lebherz, N. Marx, M. Lehrke, The sodium-glucose co-transporter-2 inhibitor ertugliflozin modifies the signature of cardiac substrate metabolism and reduces cardiac mTOR signalling, endoplasmic reticulum stress and apoptosis, Diabetes Obes. Metab. 24 (11) (2022) 2263–2272, https://doi.org/10.1111/dom.14814.
[33] D. Croteau, I. Luptak, J.M. Chambers, I. Hobai, M. Panagia, D.R. Pimentel, D. A. Siwik, F. Qin, W.S. Colucci, Effects of sodium-glucose linked transporter 2 inhibition with Ertugliflozin on mitochondrial function, energetics, and metabolic gene expression in the presence and absence of diabetes mellitus in mice, J. Am. Heart Assoc. 10 (13) (2021) e019995, https://doi.org/10.1161/JAHA.120.019995.
[34] B. Pang, L.L. Zhang, B. Li, F.X. Sun, Z.D. Wang, The sodium glucose co-transporter 2 inhibitor ertugliflozin for Alzheimer's disease: inhibition of brain insulin signaling disruption-induced tau hyperphosphorylation, Physiol. Behav. 263 (2023) 114134, https://doi.org/10.1016/j.physbeh.2023.114134.
[35] Institute of Laboratory Animal Resources, Guide for the Care and Use of Laboratory Animals, National Academy Press, 1996.
[36] N.A. Soliman, W.A. Keshk, F.H. Rizk, M.A. Ibrahim, The possible ameliorative effect of simvastatin versus sulfasalazine on acetic acid induced ulcerative colitis in adult rats, Chem. Biol. Interact. 298 (2019) 57–65, https://doi.org/10.1016/j.cbi.2018.11.002.
[37] R.M. Salama, S.F. Darwish, I. El Shaffei, N.F. Elmongy, N.M. Fahmy, M.S. Afifi, G. A. Abdel-Latif, Morus macroura Miq., Fruit extract protects against acetic acid-induced ulcerative colitis in rats: novel mechanistic insights on its impact on miRNA-223 and on the TNFα/NFκB/NLRP3 inflammatory axis, Food Chem. Toxicol. 165 (2022) 113146, https://doi.org/10.1016/j.fct.2022.113146.
[38] V. Mascitti, T.S. Maurer, R.P. Robinson, J. Bian, C.M. Boustany-Kari, T. Brandt, B. M. Collman, A.S. Kalgutkar, M.K. Klenotic, M.T. Leininger, A. Lowe, R.J. Maguire, V.M. Masterson, Z. Miao, E. Mukaiyama, J.D. Patel, J.C. Pettersen, C. Preville, B. Samas, L. She, Z. Sobol, C.M. Steppan, B.D. Stevens, B.A. Thuma, M. Tugnait, D. Zeng, T. Zhu, Discovery of a clinical candidate from the structurally unique dioxa-bicyclo[3.2.1]octane class of sodium-dependent glucose cotransporter 2 inhibitors, J. Med. Chem. 54 (8) (2011) 2952–2960, https://doi.org/10.1021/jm200049r.
[39] A.S. Kalgutkar, M. Tugnait, T. Zhu, E. Kimoto, Z. Miao, V. Mascitti, X. Yang, B. Tan, R.L. Walsky, J. Chupka, B. Feng, R.P. Robinson, Preclinical species and human disposition of PF-04971729, a selective inhibitor of the sodium-dependent glucose cotransporter 2 and clinical candidate for the treatment of type 2 diabetes mellitus, Drug Metab. Dispos. 39 (9) (2011) 1609–1619, https://doi.org/10.1124/dmd.111.040675.
[40] E.A. Elhefnawy, H.F. Zaki, N.N. El Maraghy, K.A. Ahmed, E.A. Abd El-Haleim, Genistein and/or sulfasalazine ameliorate acetic acid-induced ulcerative colitis in rats via modulating INF-gamma/JAK1/STAT1/IRF-1, TLR-4/NF-kappaB/IL-6, and JAK2/STAT3/COX-2 crosstalk, Biochem. Pharmacol. 214 (2023) 115673, https://doi.org/10.1016/j.bcp.2023.115673.
[41] M. Rafeeq, H.A.S. Murad, H.M. Abdallah, A.M. El-Halawany, Protective effect of 6-paradol in acetic acid-induced ulcerative colitis in rats, BMC Complement Med Ther 21 (1) (2021) 28, https://doi.org/10.1186/s12906-021-03203-7.
[42] G. Owusu, D.D. Obiri, G.K. Ainooson, N. Osafo, A.O. Antwi, B.M. Duduyemi, C. Ansah, Acetic acid-induced ulcerative colitis in Sprague Dawley rats is suppressed by Hydroethanolic extract of Cordia vignei leaves through reduced serum levels of TNF-alpha and IL-6, Int J Chronic Dis 2020 (2020) 8785497, https://doi.org/10.1155/2020/8785497.
[43] A. Koc, M. Duru, H. Ciralik, R. Akcan, S. Sogut, Protective agent, erdosteine, against cisplatin-induced hepatic oxidant injury in rats, Mol. Cell. Biochem. 278 (1–2) (2005) 79–84, https://doi.org/10.1007/s11010-005-6630-z.
[44] M.R. Fouad, R.M. Salama, H.F. Zaki, A.E. El-Sahar, Vildagliptin attenuates acetic acid-induced colitis in rats via targeting PI3K/Akt/NFkappaB, Nrf2 and CREB signaling pathways and the expression of lncRNA IFNG-AS1 and miR-146a, Int. Immunopharmacol. 92 (2021) 107354, https://doi.org/10.1016/j.intimp.2020.107354.
[45] E.D. Kiefer, Detection of occult blood in feces, Am. J. Surg. 25 (3) (1934) 530–535, https://doi.org/10.1016/S0002-9610(34)90223-3.
[46] S.M. Soliman, W. Wadie, S.A. Shouman, A.A. Ainshoka, Sodium selenite ameliorates both intestinal and extra-intestinal changes in acetic acid-induced colitis in rats, Naunyn Schmiedebergs Arch. Pharmacol. 391 (2018) 639–647, https://doi.org/10.1007/s00210-018-1491-7.
[47] M. Shalaby, R.R. Abdelaziz, H.A. Ghoneim, G.M. Suddek, Imatinib mitigates experimentally-induced ulcerative colitis: possible contribution of NF-kB/JAK2/STAT3/COX2 signaling pathway, Life Sci. 321 (2023) 121596, https://doi.org/10.1016/j.lfs.2023.121596.
[48] M.A. Bejeshk, A.H. Aminizadeh, M.A. Rajizadeh, M. Khaksari, M. Lashkarizadeh, N. Shahrokhi, M.J. Zahedi, M. Azimi, The effect of combining basil seeds and gum Arabic on the healing process of experimental acetic acid-induced ulcerative colitis in rats, J. Tradit. Complement. Med. 12 (6) (2022) 599–607, https://doi.org/10.1016/j.jtcme.2022.08.001.
[49] I.A. Alsharif, H.M. Fayed, R.F. Abdel-Rahman, R.M. Abd-Elsalam, H.A. Ogaly, Miconazole mitigates acetic acid-induced experimental colitis in rats: insight into inflammation, oxidative stress and Keap1/Nrf-2 signaling crosstalk, Biology 11 (2) (2022) 303, https://doi.org/10.3390/biology11020303.
[50] S. Saber, R.M. Khalil, W.S. Abdo, D. Nassif, E. El-Ahwany, Olmesartan ameliorates chemically-induced ulcerative colitis in rats via modulating NFkappaB and Nrf-2/HO-1 signaling crosstalk, Toxicol. Appl. Pharmacol. 364 (2019) 120–132, https://doi.org/10.1016/j.taap.2018.12.020.
[51] P. Trinder, Determination of blood glucose using 4-amino phenazone as oxygen acceptor, J. Clin. Pathol. 22 (2) (1969) 246.
[52] K.J. Livak, T.D. Schmittgen, Analysis of relative gene expression data using real-time quantitative PCR and the 2(-Delta Delta C(T)) method, Methods 25 (4) (2001) 402–408, https://doi.org/10.1006/meth.2001.1262.
[53] M.M. Bradford, A rapid and sensitive method for the quantitation of microgram quantities of protein utilizing the principle of protein-dye binding, Anal. Biochem. 72 (1) (1976) 248–254, https://doi.org/10.1016/0003-2697(76)90527-3.
[54] C.F.A. Culling, Handbook of histopathological and histochemical techniques: including museum techniques, Butterworth-Heinemann2013.
[55] L.H. Khedr, R.M. Eladawy, N.N. Nassar, M.A.E. Saad, Canagliflozin attenuates chronic unpredictable mild stress induced neuroinflammation via modulating AMPK/mTOR autophagic signaling, Neuropharmacology 223 (2023) 109293, https://doi.org/10.1016/j.neuropharm.2022.109293.
[56] M. Nasr, S. Cavalu, S. Saber, M.E. Youssef, A.M. Abdelhamid, H.I. Elagamy, I. Kamal, A.G.A. Gaafar, E. El-Ahwany, N.A. Amin, Canagliflozin-loaded chitosan-hyaluronic acid microspheres modulate AMPK/NF-κB/NLRP3 axis: a new paradigm in the rectal therapy of ulcerative colitis, Biomed. Pharmacother. 153 (2022) 113409, https://doi.org/10.1016/j.biopha.2022.113409.
[57] M.A. El-Rous, S. Saber, E.M. Raafat, A.A.E. Ahmed, Dapagliflozin, an SGLT2 inhibitor, ameliorates acetic acid-induced colitis in rats by targeting NFkappaB/AMPK/NLRP3 axis, Inflammopharmacology 29 (4) (2021) 1169–1185, https://doi.org/10.1007/s10787-021-00818-7.
[58] G. Owusu, D.D. Obiri, G.K. Ainooson, N. Osafo, A.O. Antwi, B.M. Duduyemi, C. Ansah, Acetic acid-induced ulcerative colitis in Sprague dawley rats is suppressed by hydroethanolic extract of Cordia vignei leaves through reduced serum levels of TNF-α and IL-6, Int J Chronic Dis 2020 (1) (2020) 8785497, https://doi.org/10.1155/2020/8785497.
[59] T. Kobayashi, B. Siegmund, C. Le Berre, S.C. Wei, M. Ferrante, B. Shen, C. N. Bernstein, S. Danese, L. Peyrin-Biroulet, T. Hibi, Ulcerative colitis (primer), Nat. Rev. Dis. Primers. 6 (1) (2020) 74.
[60] J. Long, X.K. Liu, Z.P. Kang, M.X. Wang, H.M. Zhao, J.Q. Huang, Q.P. Xiao, D. Y. Liu, Y.B. Zhong, Ginsenoside Rg1 ameliorated experimental colitis by regulating the balance of M1/M2 macrophage polarization and the homeostasis of intestinal flora, Eur. J. Pharmacol. 917 (2022) 174742, https://doi.org/10.1016/j.ejphar.2022.174742.
[61] M.M. Wu, Q.M. Wang, B.Y. Huang, C.T. Mai, C.L. Wang, T.T. Wang, X.J. Zhang, Dioscin ameliorates murine ulcerative colitis by regulating macrophage polarization, Pharmacol. Res. 172 (2021) 105796, https://doi.org/10.1016/j.phrs.2021.105796.
[62] F. Deng, J. Yan, J. Lu, M. Luo, P. Xia, S. Liu, X. Wang, F. Zhi, D. Liu, M2 macrophage-derived Exosomal miR-590-3p attenuates DSS-induced mucosal damage and promotes epithelial repair via the LATS1/YAP/ β-catenin Signalling Axis, J. Crohn's Colitis 15 (4) (2020) 665–677, https://doi.org/10.1093/ecco-jcc/jjaa214.
[63] P. Marincola Smith, Y.A. Choksi, N.O. Markham, D.N. Hanna, J. Zi, C.J. Weaver, J. A. Hamaamen, K.B. Lewis, J. Yang, Q. Liu, I. Kaji, A.L. Means, R.D. Beauchamp, Colon epithelial cell TGFβ signaling modulates the expression of tight junction proteins and barrier function in mice, American journal of physiology-gastrointestinal and liver, Physiology 320 (6) (2021) G936–G957, https://doi.org/10.1152/ajpgi.00053.2021.

[64] T. Liu, L. Zhang, D. Joo, S.C. Sun, NF-kappaB signaling in inflammation, Signal Transduct. Target. Ther. 2 (2017) 17023, https://doi.org/10.1038/sigtrans.2017.23.
[65] G. Xu, L. Feng, P. Song, F. Xu, A. Li, Y. Wang, Y. Shen, X. Wu, Q. Luo, X. Wu, Isomeranzin suppresses inflammation by inhibiting M1 macrophage polarization through the NF-κB and ERK pathway, Int. Immunopharmacol. 38 (2016) 175–185, https://doi.org/10.1016/j.intimp.2016.05.027.
[66] Q. Lv, Y. Xing, Y. Liu, Q. Chen, J. Xu, L. Hu, Y. Zhang, Didymin switches M1-like toward M2-like macrophage to ameliorate ulcerative colitis via fatty acid oxidation, Pharmacol. Res. 169 (2021) 105613, https://doi.org/10.1016/j.phrs.2021.105613.
[67] T. Sun, C.H.T. Kwong, C. Gao, J. Wei, L. Yue, J. Zhang, R.D. Ye, R. Wang, Amelioration of ulcerative colitis via inflammatory regulation by macrophage-biomimetic nanomedicine, Theranostics 10 (22) (2020) 10106–10119, https://doi.org/10.7150/thno.48448.
[68] J. Wang, X. Zhao, Q. Wang, X. Zheng, D. Simayi, J. Zhao, P. Yang, Q. Mao, H. Xia, FAM76B regulates PI3K/Akt/NF-kappaB-mediated M1 macrophage polarization by influencing the stability of PIK3CD mRNA, Cell. Mol. Life Sci. 81 (1) (2024) 107, https://doi.org/10.1007/s00018-024-05133-2.
[69] A. Abd Uljaleel, E. Hassan, Protective effect of ertugliflozin against acute lung injury caused by endotoxemia model in mice, Iranian journal of war and public, Health 15 (1) (2023) 67–75.
[70] R.T. Kareem, M.K. Abass, A potential anti-inflammatory effect of Ertugliflozin in animal model, South Asian Res J Pharm Sci 6 (3) (2024) 84–88.
[71] M.Y. Li, Y.Z. Wu, J.G. Qiu, J.X. Lei, M.X. Li, N. Xu, Y.H. Liu, Z. Jin, Z.R. Su, S. M. Lee, X.B. Zheng, H. Xiao-Qi, Huangqin decoction ameliorates ulcerative colitis by regulating fatty acid metabolism to mediate macrophage polarization via activating FFAR4-AMPK-PPARalpha pathway, J. Ethnopharmacol. 311 (2023) 116430, https://doi.org/10.1016/j.jep.2023.116430.
[72] L. Xu, N. Nagata, M. Nagashimada, F. Zhuge, Y. Ni, G. Chen, E. Mayoux, S. Kaneko, T. Ota, SGLT2 inhibition by Empagliflozin promotes fat utilization and Browning and Attenuates inflammation and insulin resistance by polarizing M2 macrophages in diet-induced obese mice, EBioMedicine 20 (2017) 137–149, https://doi.org/10.1016/j.ebiom.2017.05.028.
[73] T.M. Lee, N.C. Chang, S.Z. Lin, Dapagliflozin, a selective SGLT2 inhibitor, attenuated cardiac fibrosis by regulating the macrophage polarization via STAT3 signaling in infarcted rat hearts, Free Radic. Biol. Med. 104 (2017) 298–310, https://doi.org/10.1016/j.freeradbiomed.2017.01.035.
[74] S. Qu, Y. Shen, M. Wang, X. Wang, Y. Yang, Suppression of miR-21 and miR-155 of macrophage by cinnamaldehyde ameliorates ulcerative colitis, Int. Immunopharmacol. 67 (2019) 22–34, https://doi.org/10.1016/j.intimp.2018.11.045.
[75] J. Zeng, D. Zhang, X. Wan, Y. Bai, C. Yuan, T. Wang, D. Yuan, C. Zhang, C. Liu, Chlorogenic acid suppresses miR-155 and ameliorates ulcerative colitis through the NF-kappaB/NLRP3 Inflammasome pathway, Mol. Nutr. Food Res. 64 (23) (2020) e2000452, https://doi.org/10.1002/mnfr.202000452.
[76] J. Wan, L. Xia, W. Xu, N. Lu, Expression and function of miR-155 in diseases of the gastrointestinal tract, Int. J. Mol. Sci. 17 (5) (2016) 709, https://doi.org/10.3390/ijms17050709.
[77] J. Wan, L. Xia, W. Xu, N. Lu, Expression and function of miR-155 in diseases of the gastrointestinal tract, Int. J. Mol. Sci. 17 (5) (2016) 709, https://doi.org/10.3390/ijms17050709.
[78] G. Liu, E. Abraham, MicroRNAs in immune response and macrophage polarization, Arterioscler. Thromb. Vasc. Biol. 33 (2) (2013) 170–177, https://doi.org/10.1161/ATVBAHA.112.300068.
[79] Z.B. Yang, L.Z. Qiu, Q. Chen, J.D. Lin, Artesunate alleviates the inflammatory response of ulcerative colitis by regulating the expression of miR-155, Pharm. Biol. 59 (1) (2021) 97–105, https://doi.org/10.1080/13880209.2020.1867196.
[80] J. Li, J. Zhang, H. Guo, S. Yang, W. Fan, N. Ye, Z. Tian, T. Yu, G. Ai, Z. Shen, H. He, P. Yan, H. Lin, X. Luo, H. Li, Y. Wu, Critical role of alternative M2 skewing in miR-155 deletion-mediated protection of colitis, Front. Immunol. 9 (2018) 904, https://doi.org/10.3389/fimmu.2018.00904.
[81] E. Abdollahi, F. Keyhanfar, A.A. Delbandi, R. Falak, S.J. Hajimiresmaiel, M. Shafiei, Dapagliflozin exerts anti-inflammatory effects via inhibition of LPS-induced TLR-4 overexpression and NF-kappaB activation in human endothelial cells and differentiated macrophages, Eur. J. Pharmacol. 918 (2022) 174715, https://doi.org/10.1016/j.ejphar.2021.174715.
[82] F.R. Alsereidi, Z. Khashim, H. Marzook, A. Gupta, A.M. Al-Rawi, M.M. Ramadan, M.A. Saleh, Targeting inflammatory signaling pathways with SGLT2 inhibitors: insights into cardiovascular health and cardiac cell improvement, Curr. Probl. Cardiol. 49 (5) (2024) 102524, https://doi.org/10.1016/j.cpcardiol.2024.102524.
[83] Y. Shen, J. Zou, M. Chen, Z. Zhang, C. Liu, S. Jiang, D. Qian, J.A. Duan, Protective effects of Lizhong decoction on ulcerative colitis in mice by suppressing inflammation and ameliorating gut barrier, J. Ethnopharmacol. 259 (2020) 112919, https://doi.org/10.1016/j.jep.2020.112919.
[84] Y.X. He, Y.Y. Li, Y.Q. Wu, L.Z. Ren, Y. Wang, Y.M. Wang, Y. Yu, Huanglian Ganjiang decoction alleviates ulcerative colitis by restoring gut barrier via APOC1-JNK/P38 MAPK signal pathway based on proteomic analysis, J. Ethnopharmacol. 318 (Pt B) (2024) 116994, https://doi.org/10.1016/j.jep.2023.116994.
[85] D.D. Ren, K.C. Chen, S.S. Li, Y.T. Zhang, Z.M. Li, S. Liu, Y.S. Sun, Panax quinquefolius polysaccharides ameliorate ulcerative colitis in mice induced by dextran sulfate sodium, Front. Immunol. 14 (2023) 1161625, https://doi.org/10.3389/fimmu.2023.1161625.
[86] Y. Zhao, H. Chen, W. Li, Q. He, J. Liang, X. Yan, Y. Yuan, T. Yue, Selenium-containing tea polysaccharides ameliorate DSS-induced ulcerative colitis via enhancing the intestinal barrier and regulating the gut microbiota, Int. J. Biol. Macromol. 209 (Pt A) (2022) 356–366, https://doi.org/10.1016/j.ijbiomac.2022.04.028.
[87] L. Zhu, P. Gu, H. Shen, Protective effects of berberine hydrochloride on DSS-induced ulcerative colitis in rats, Int. Immunopharmacol. 68 (2019) 242–251, https://doi.org/10.1016/j.intimp.2018.12.036.
[88] Y. Wang, J. Zhang, B. Zhang, M. Lu, J. Ma, Z. Liu, J. Huang, J. Ma, X. Yang, F. Wang, X. Tang, Modified Gegen Qinlian decoction ameliorated ulcerative colitis by attenuating inflammation and oxidative stress and enhancing intestinal barrier function in vivo and in vitro, J. Ethnopharmacol. 313 (2023) 116538, https://doi.org/10.1016/j.jep.2023.116538.
[89] C. Li, Y. Jiao, S. Shen, W. Zhao, Q. Zhang, S. Zhang, Chaenomeles sinensis polysaccharide and its carboxymethylated derivative alleviate dextran sulfate sodium-induced ulcerative colitis via suppression of inflammation and oxidative stress, Biomed. Pharmacother. 169 (2023) 115941, https://doi.org/10.1016/j.biopha.2023.115941.
[90] A. Shawky, S. Saber, E.M. Abd El-Kader, H.A. El-Kashef, Verapamil inhibits TXNIP-dependent NLRP3 Inflammasome activation in an ulcerative colitis rat model: a new evolving role of the calcium channel blocker, Int. Immunopharmacol. 158 (2025) 114751, https://doi.org/10.1016/j.intimp.2025.114751.
[91] H.A. Hassan, A. Mohamed abdelhamid, W. Samy, H. Osama Mohammed, S. Mortada Mahmoud, A. Fawzy Abdel Mageed, N.A.T. Abbas, Ameliorative effects of androstenediol against acetic acid-induced colitis in male wistar rats via inhibiting TLR4-mediated PI3K/Akt and NF-κB pathways through estrogen receptor β activation, Int. Immunopharmacol. 127 (2024) 111414.doi:doi:https://doi.org/10.1016/j.intimp.2023.111414.
[92] M.J. Manna, A. Abu-raghif, H.Y. Muhsin, The effect of Niclosamide in acetic acid induce colitis: an experimental study, Prensa méd. argent (2019) 309–316.
[93] N.H. Hassan, G.M. Kamel, H.M. Fayed, R.M.S. Korany, A. Ramadan, Ertugliflozin, a SGLT-2 inhibitor, guards against Thioacetamide-induced liver fibrosis: the Nrf2/HO-1 and TLR4/ TGF-β1 pathways, J. Appl. Veterinary Sci. 10 (3) (2025) 34–47, https://doi.org/10.21608/javs.2025.372525.1573.
[94] G.A. Albalawi, M.Z. Albalawi, K.T. Alsubaie, A.Z. Albalawi, M.A.F. Elewa, K. S. Hashem, M.M.H. Al-Gayyar, Curative effects of crocin in ulcerative colitis via modulating apoptosis and inflammation, Int. Immunopharmacol. 118 (2023) 110138, https://doi.org/10.1016/j.intimp.2023.110138.
[95] M. El-Sherbiny, N.H. Eisa, N.F. Abo El-Magd, N.M. Elsherbiny, E. Said, A.E. Khodir, Anti-inflammatory/anti-apoptotic impact of betulin attenuates experimentally induced ulcerative colitis: an insight into TLR4/NF-kB/caspase signalling modulation, Environ. Toxicol. Pharmacol. 88 (2021) 103750, https://doi.org/10.1016/j.etap.2021.103750.
[96] C. Liu, Y. Zeng, Y. Wen, X. Huang, Y. Liu, Natural products modulate cell apoptosis: a promising way for the treatment of ulcerative colitis, Front. Pharmacol. 13 (2022) 806148, https://doi.org/10.3389/fphar.2022.806148.
[97] H.A.A. Elmaksoud, M.H. Motawea, A.A. Desoky, M.G. Elharrif, A. Ibrahimi, Hydroxytyrosol alleviate intestinal inflammation, oxidative stress and apoptosis resulted in ulcerative colitis, Biomed. Pharmacother. 142 (2021) 112073, https://doi.org/10.1016/j.biopha.2021.112073.
[98] F.R. Jaafar, A. Abu-Raghif, Comparative treatment of sulfasalazine+ ezetimibe combination and sulfasalazine in a rat model with induced colitis, J. Med. Life 16 (8) (2023) 1165, https://doi.org/10.25122/jml-2023-0194.